

RAL IASI Methane Retrieval

ATBD



Science and
Technology
Facilities Council

RAL Space

Prepared by

L. Ventress

R. Siddans

D. Knappett

RAL Space

Remote Sensing Group

Harwell Campus

Didcot, OX11 0QX

United Kingdom

ESA Methane+

2022-07-21



CONTENTS

Acronyms.....	3
1 Introduction.....	5
1.1 Purpose	5
1.2 Scope.....	5
2 References	6
2.1 Reference documents	6
2.2 Electronic references	8
3 Algorithm Description.....	9
3.1 Heritage.....	9
3.2 Overview	9
3.3 Optimal Estimation	11
3.4 Measurements.....	12
3.4.1 IASI.....	12
3.4.2 Selection of IASI Observations	14
3.4.3 Measurement Errors.....	14
3.5 Forward Model.....	16
3.6 State vector	16
3.6.1 Use of IMS DATA.....	18
3.6.2 Use of ECMWF Data.....	19
3.6.3 Methane a priori	19
3.6.4 Water Vapour	20
3.7 Modelling N ₂ O.....	22
3.8 Fitting of Systematic Residual Patterns.....	23
4 Retrieval Scheme Characterisation and Error Analysis.....	25
5 Candidate V3 Algorithm.....	31



5.1	Overview	31
5.2	Use of IMS data	31
5.3	Measurements	33
5.4	Forward Model.....	33
5.5	State Vector.....	33
5.5.1	Surface emissivity	33
5.5.2	Surface temperature.....	34
5.5.3	Methane a priori	34
5.6	Additional minor trace gases	34
5.7	Modelling N2O	36
5.8	Fitting of Systematic Residual Patterns.....	37
6	L2 Product.....	39
6.1	Overview	39
6.2	L2 File name	39
6.3	Format and content	40
6.3.1	Data Dimensions	40
6.3.2	Global Attributes.....	40
6.3.3	Variables	41




ACRONYMS

ATBD	Algorithm Theoretical Basis Document
AVHRR	Advanced Very High Resolution Radiometer
CEDA	UK Centre for Environmental Data Analysis
CH4	Methane
DOFS	Degrees of Freedom for Signal
ECMWF	European Centre for Medium-Range Weather Forecasts
ESA	European Space Agency
ESD	Estimated Standard Deviation (estimated random uncertainty of a retrieved quantity)
EUMETSAT	European Organization for the Exploitation of Meteorological Satellites
FM	Forward Model
GOSAT	Greenhouse Gases Observing Satellite
HITRAN	High Resolution Transmission
IASI	Infrared Atmospheric Sounding Interferometer
IR	Infrared
LBL	Line-By-Line
LBLRTM	Line-By-Line Radiative Transfer Model
L1	Level 1
L2	Level 2
LUT	Look-up-table
MACC	Monitoring Atmospheric Composition and Climate
Metop	Meteorological operational satellite
NCEO	National Centre for Earth Observation
NEBT	Noise Equivalent Brightness Temperature
NRT	Near Real Time
N2O	Nitrous oxide



OE	Optimal Estimation
OEM	Optimal Estimation Method
PC	Principle Components
PCA	Principle Components Analysis
PV	Potential Vorticity
RAL	Rutherford Appleton Laboratory
RFM	(University of Oxford) Reference Forward Model
RSG	Remote Sensing Group
RTM	Radiative Transfer Model
RTTOV	Radiative Transfer for TOVS
SWIR	Short-wave infrared
STFC	Science and Technology Facilities Council
TCCON	Total Column Carbon Observing Network
TOMCAT	Toulouse Off-line Model of Chemistry And Transport
VMR	Volume mixing ratio
WP	Work Package

 UKRI Science and Technology Facilities Council RAL Space	RAL IASI Methane Retrieval ATBD Version 2.1	2022-07-21
		Page 5 of 42

1 INTRODUCTION


1.1 PURPOSE

This is the algorithm theoretical basis document (ATBD) for the Rutherford Appleton Laboratory (RAL) Remote Sensing Group (RSG) thermal infrared (TIR) IASI methane retrieval scheme. The purpose of this document is to provide a detailed mathematical and physical description of the algorithm, as well as describing the schemes inputs, outputs, and data products.

1.2 SCOPE

This document describes version 2.0 of the RAL IASI methane retrieval scheme. The algorithm was developed by RAL through its role in the UK National Centre for Earth Observation (NCEO) (RD-1), with additional support from Eumetsat (RD-14, RD-13). This ATBD was produced in the framework of the ESA Methane+ project, to provide a consolidated description of the scheme, based on existing relevant documentation (RD-14, RD-13, RD-16).

Within the ESA Methane+ project the “version 2” RAL scheme was used to produce a “Methane+ version 1 TIR” dataset from Metop B between January 2018 and March 2021, supplementing the previously generated, publicly available dataset for Metop A (from June 2007 onwards). Further development of the scheme took place leading to the definition of a “candidate version 3 algorithm”, used to produce a “Methane+ version 2” dataset. This ATBD describes in detail the version 2.0 algorithm and the outlines the differences between this and the new candidate version 3 scheme.


 Science and Technology Facilities Council RAL Space	RAL IASI Methane Retrieval ATBD Version 2.1	2022-07-21
		Page 6 of 42

2 REFERENCES

2.1 REFERENCE DOCUMENTS

- RD-1. M. Waterfall, R. Siddans, B. J. Kerridge, G. Miles, B. G. Latter, RETRIEVAL OF METHANE DISTRIBUTIONS FROM IASI, Proceedings of ESA ATMOS 2012, European Space Agency, ESA Special Publication SP-708 (CD-ROM), 2012,
ftp://ftp.rsg.rl.ac.uk/publications/waterfall_iasiMethane_procEsaAtmosSciConf_2012.pdf
- RD-2. Rodgers, C.D., Inverse Methods for Atmospheric Sounding: Theory and Practice, World Sci., Hackensack, N.J. 2000.
- RD-3. Press, W.H., Teukolsky, S., Vetterling, W.T. and Flannery, B., Numerical Recipes: the art of scientific computing, Second edition, Cambridge University Press, 1995.
- RD-4. Seemann, Suzanne W., Eva E. Borbas, Robert O. Knuteson, Gordon R. Stephenson, Hung-Lung Huang, 2008: Development of a Global Infrared Land Surface Emissivity Database for Application to Clear Sky Sounding Retrievals from Multispectral Satellite Radiance Measurements. *J. Appl. Meteor. Climatol.*, 47, 108–123
- RD-5. Rothman et al, The HITRAN 2008molecularspectroscopicdatabase, *Journal of Quantitative Spectroscopy and Radiative Transfer*, vol. 110, pp. 533-572 (2009).
- RD-6. A. Razavi, C. Clerbaux, C. Wespes, L. Clarisse, D. Hurtmans, S. Payan, C. Camy-Peyret and P. F. Coheur, "Characterization of methane retrievals from the IASI space-borne sounder," *Atmos. Chem. Phys.*, vol. 9, pp. 7889-7899, 2009
- RD-7. D. Blumstein ; B. Tournier ; F. R. Cayla ; T. Phulpin ; R. Fjortoft ; C. Buil ; G. Ponce, In-flight performance of the infrared atmospheric sounding interferometer (IASI) on METOP-A Proc. SPIE 6684, (24 September 2007); doi: 10.1117/12.734162
- RD-8. Siddans, R.: Fast transmittance modelling of the MSG and MTG solar channels for cloud retrievals, Eumetsat Study Final report, 2011.
http://eumeds.eumetsat.int/groups/ops/documents/document/pdf_report_fast_trans.pdf
- RD-9. Chipperfield, M.P., B.V. Khattatov, and D.J. Lary, Sequential Assimilation of Stratospheric Chemical Observations in a Three-Dimensional Model, *J. Geophys. Res.*, 107(D21), 4585, doi:10.1029/2002JD002110, 2002.
- RD-10. D. Lary. Lagrangian four dimensional variational data assimilation of chemical species. *The Quarterly Journal of the Royal Meteorological Society*, 121, 704., 1995.
- RD-11. B.J. Hoskins. The role of potential vorticity in symmetric stability and instability. *Quarterly Journal of the Royal Meteorological Society*, 100, pp. 480-482., 1974.
- RD-12. Jones, A., Technical Note: A trace gas climatology derived from the Atmospheric Chemistry Experiment Fourier Transform Spectrometer dataset, *Atmos. Chem. Phys.*, 12, 5207-5220, doi:10.5194/acp-12-5207-2012
- RD-13. Knappett, D., Siddans, R., Walker, J., and Kerridge, B.: Rider to: IASI CH4 Operational Retrieval Feasibility – Optimal Estimation Method, Final Report, Eumetsat Contract, EUM/CO/14/4600001315/RM, 2018.
- RD-14. Siddans, R. and Hurley, J.: IASI CH4 Operational Retrieval Feasibility – Optimal Estimation Method: Final Report, Eumetsat Contract, EUM/CO/14/4600001315/RM, 2015.
- RD-15. Siddans, R., D. Gerber, Optimal Estimation Method Retrievals with IASI, AMSU and MHS Measurements: Eumetsat Contract EUM/CO/13/46000001252/THH, Final Report, January 2015.


- RD-16. Siddans R., Knappett, D., Kerridge, B., Waterfall, A., Hurley, J., Latter, B., Boesch, H., and Parker, R., Global height resolved methane retrievals from the Infrared Atmospheric Sounding Interferometer (IASI) on MetOp, *Atmos. Meas. Tech.*, 10, 4135-4164, <http://doi.org/10.5194/amt-10-4135-2017>, 2017.
- RD-17. Siddans, R.: Water Vapour Climate Change Initiative – Phase One: ATBD Part 2 – IMS L2 Product, ESA
- RD-18. Siddans, R.; Knappett, D.; Kerridge, B.; Latter, B.; Waterfall, A.; Hurley, J.; Walker, J. (2016): STFC RAL methane retrievals from IASI on board MetOp-A, version 1.0. Centre for Environmental Data Analysis, 18 March 2016. doi:10.5285/B6A84C73-89F3-48EC-AEE3-592FEF634E9B. <http://dx.doi.org/10.5285/B6A84C73-89F3-48EC-AEE3-592FEF634E9B>
- RD-19. Siddans, R.; Knappett, D.; Kerridge, B.; Latter, B.; Waterfall, A. (2020): STFC RAL methane retrievals from IASI on board MetOp-A, version 2.0. Centre for Environmental Data Analysis, 10 March 2020. doi:10.5285/f717a8ea622f495397f4e76f777349d1. <http://dx.doi.org/10.5285/f717a8ea622f495397f4e76f777349d1>
- RD-20. Bergamaschi, P., Houweling, S., Segers, A., Krol, M., Frankenberg, C., Scheepmaker, R. A., ... Gerbig, C. (2013). Atmospheric CH₄ in the first decade of the 21st century: Inverse modeling analysis using SCIAMACHY satellite retrievals and NOAA surface measurements. *Journal of Geophysical Research: Atmospheres*, 118(13), 7350–7369. <https://doi.org/10.1002/jgrd.50480>
- RD-21. Knappett, Diane (2019) *RAL IASI MetOp-A TIR Methane Dataset v2.0 Product User Guide*. Documentation. Centre for Environmental Data Analysis (CEDA); <http://cedadocs.ceda.ac.uk/1467/>
- RD-22. Matricardi, M.: Technical Note: An assessment of the accuracy of the RTTOV fast radiative transfer model using IASI data, *Atmos. Chem. Phys.*, 9, 6899–6913, <https://doi.org/10.5194/acp-9-6899-2009>, 2009.
- RD-23. Spectroscopy and forward model errorimprovement for CH₄ retrieval in the TIR: ESA Contract No. 4000125380/18/NL/AF. June 2021
- RD-24. Clough, S. A., M. W. Shephard, E. J. Mlawer, J. S. Delamere, M. J. Iacono, K. Cady-Pereira, S. Boukabara, and P. D. Brown, Atmospheric radiative transfer modeling: a summary of the AER codes, Short Communication, *J. Quant. Spectrosc. Radiat. Transfer*, 91, 233-244, 2005.LBLRTM
- RD-25. I.E. Gordon, L.S. Rothman, R.J. Hargreaves et al., "The HITRAN2020 molecular spectroscopic database", *Journal of Quantitative Spectroscopy and Radiative Transfer* 277, 107949 (2022).Hitran 2018
- RD-26. Koo, Ja-Ho, (2017), Global climatology based on the ACE-FTS version 3.5 data set: Addition of mesospheric levels and carbon-containing species in the UTLS, *Journal of Quantitative Spectroscopy and Radiative Transfer*, 12, 52-62, doi:10.1016/j.jqsrt.2016.07.003 (PDF)ACE version 4 climatology
- RD-27. Evaluation and Quality Control document for N₂O flux inversion 18r1 (Period covered 1996 to year 2018) D3.4.1-2018; Issued by: CEA / Frédéric Chevallier; Date: 25/01/2021; Ref: CAMS73_2018SC2_D3.4.1-2018_202101
- RD-28. Houweling, S., Bergamaschi, P., Chevallier, F., Heimann, M., Kaminski, T., Krol, M., Michalak, A. M., and Patra, P.: Global inverse modeling of CH₄ sources and sinks: an overview of methods, *Atmos. Chem. Phys.*, 17, 235–256, <https://doi.org/10.5194/acp-17-235-2017>, 2017.CAMS CH₄ flux inversion v19r1
- RD-29. Saunders, R. et al, RTTOV-12 Science and Validation Report; Doc ID : NWPSAF-MO-TV-41; Version : 1.0; 16/02/2017
- RD-30. Hocking, J., RTTOV v12 Users Guide; Doc ID : NWPSAF-MO-UD-037; Version : 1.2; 03/04/2018

 RAL Space	RAL IASI Methane Retrieval ATBD Version 2.1	2022-07-21
		Page 8 of 42

RD-31. Prunet, P et al, Spectroscopy and forward model error; improvement for CH4 retrieval in the TIR; Executive Summary; SPA-022-TN-005 - Issue 1 - Revision 0; ESA Contract No. 4000125380/18/NL/AF; 9 June 2021

2.2 ELECTRONIC REFERENCES

- ER-1. <http://www.atm.ox.ac.uk/RFM/>
- ER-2. <http://www.see.leeds.ac.uk/tomcat/>
- ER-3. <https://lta.cr.usgs.gov/GTOPO30>
- ER-4. <https://www.esrl.noaa.gov/gmd/>

 UKRI Science and Technology Facilities Council	RAL IASI Methane Retrieval ATBD Version 2.1	2022-07-21
		Page 9 of 42

3 ALGORITHM DESCRIPTION

3.1 HERITAGE

The RAL IASI methane retrieval scheme was developed by the RAL Remote Sensing Group in earlier work for the UK National Centre for Earth Observation (NCEO). The original (version 1.0) algorithm was extensively evaluated in the Eumetsat study “IASI CH₄ Operational Retrieval Feasibility – Optimal Estimation Method” (RD-14) and published in RD-16. The dataset was archived with the Centre for Environmental Data Analysis (CEDA) in 2016 (RD-18), providing global, height-resolved atmospheric methane data for public use.

Further developments, leading to the development of the version 2.0 scheme described in this ATBD, were explored in a follow-on study (RD-13). The new scheme improves on version 1.0 by using results from the RAL Infrared and Microwave Sounder (IMS) scheme (RD-15, RD-17) to define temperature profiles and surface emissivity (instead of taking these from ECMWF analysis). The new scheme also introduces a latitude dependence in the assumed *a priori* tropospheric methane and fits the isotopic ratio of 13-CH₄. The version 2.0 dataset contains 10 years (2007-2017) of global methane retrievals and was archived in 2020 (RD-18).

3.2 OVERVIEW

The methane (CH₄) retrieval scheme is based on the optimal estimation method (OEM), which solves an otherwise under-constrained inverse problem by introducing prior information. The algorithm is applied to data from the IASI instruments on board Metop A, B and C in the spectral range 1232.25-1290 cm⁻¹, to produce global height-resolved CH₄ estimates. The algorithm jointly fits methane with other parameters including water vapour (main isotope and HDO separately), surface temperature, cloud fraction and cloud altitude.

The retrieval of (effective) cloud parameters is possible through the exploitation of nitrous oxide (N₂O) spectral features within the fit window (which have comparable strength to that of methane). This approach has been extremely effective in mitigating errors in the methane retrieval caused by the presence of optically thin cloud, partial cloud cover, and other geophysical variables.

The RTTOV forward model (currently v10.2) is used in the retrieval scheme with customised coefficients that have been derived at RAL specifically for this application.

Collocated values of temperature, water vapour, and surface spectral emissivity, required as prior information, are pre-retrieved using the RAL IMS retrieval scheme which was developed at RAL during the study “Optimal Estimation Method retrievals with IASI, AMSU and MHS measurements” (RD-15, RD-17).

By fitting IASI measured spectra to an RMS in brightness temperature of order 0.1 K, the scheme delivers CH₄ column average mixing ratios with a precision of around 20 ppbv. To achieve this level of fitting precision, it has been necessary to derive in-house a model of the IASI noise-equivalent brightness temperature (NEBT) which better represents the photometric noise in the 1250-1290 cm⁻¹ spectral region than the nominal IASI NEBT model. In this spectral range the noise on a given spectrum is strongly affected by scene photon noise (i.e. dependent on the band-integrated scene radiance).

At this fitting precision, retrieval diagnostics from the RAL OE scheme indicate there to be >2 degrees of freedom for signal (see Figure 1), which is supported by comparisons of retrieved distributions at several different pressure levels with those from chemical transport models.

Without correction, the scheme generates methane mixing ratios that are biased by about 5% with some scan angle dependence. This is currently corrected by (a) scaling assumed methane line strengths by a factor of 1.04, and by (b) jointly fitting a scale factor for a (time/space invariant) systematic spectral pattern which is itself derived to minimise the across track variations in methane over the Southern hemisphere oceans. These corrections are assumed to be necessary to compensate for forward model errors - in particular errors in spectroscopy and modelling of the CH₄ line shape.

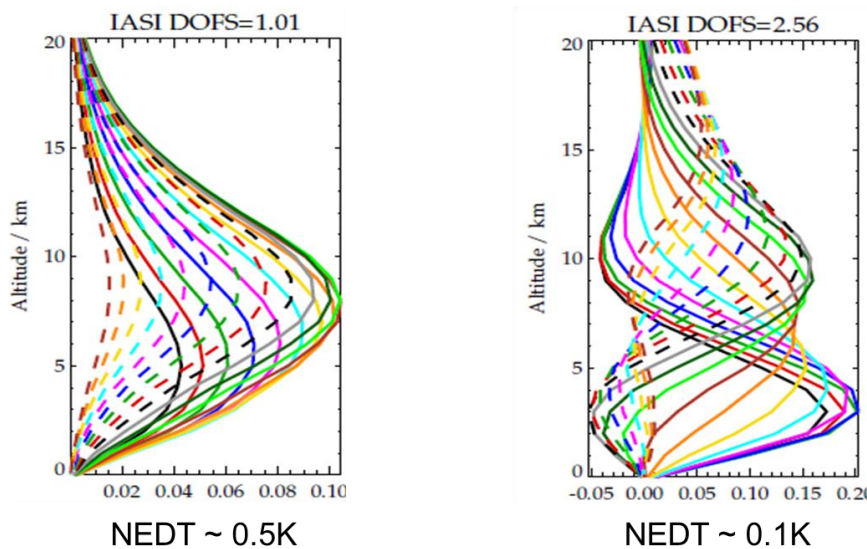


Figure 1: Averaging kernels for IASI retrievals of CH₄ from the RAL fit window (typical mid-latitude conditions). These characterise the vertical sensitivity of each retrieval level to perturbations in the true profile of methane. The panel on the left shows kernels for a noise equivalent brightness temperature of 0.5K, from which the degrees of freedom for signal (DOFS) are around 1. With a fit precision of 0.1K (panel on right) this increases to 2.56, and so two distinct layers in the troposphere / lower stratosphere can be resolved.

 UKRI Science and Technology Facilities Council	RAL IASI Methane Retrieval ATBD Version 2.1	2022-07-21
		Page 11 of 42

3.3 OPTIMAL ESTIMATION

The retrieval scheme uses the standard optimal estimation method (RD-2). This solves the otherwise under-constrained inverse problem of determining atmospheric composition from radiance spectra by introducing prior information in a statistically optimal manner, by finding the state which minimises the cost function:

$$\chi^2 = (\mathbf{y} - F(\mathbf{x}))^T \mathbf{S}_y^{-1} (\mathbf{y} - F(\mathbf{x})) + (\mathbf{a} - \mathbf{x})^T \mathbf{S}_a^{-1} (\mathbf{a} - \mathbf{x})$$

Equation 1

where

- \mathbf{y} is a measurement vector containing each measured value used by the retrieval
- \mathbf{S}_y is the measurement covariance matrix, describing the expected errors on each measurement.
- \mathbf{x} is the state vector containing estimates of each retrieved parameter
- \mathbf{a} is an *a priori* estimate of the state
- \mathbf{S}_a is the *a priori* covariance matrix, which describes expected errors in the *a priori* estimate of the state.
- $F(\mathbf{x})$ is the *forward model*, a function which estimates the measured values, given defined values of the state.


The solution which minimises this cost function is found using the Levenburg-Marquardt method (summarised in RD-3). This finds the solution iteratively applying the following equation until convergence is achieved.

$$\mathbf{x}_{i+1} = \mathbf{x}_i + (\mathbf{S}_a^{-1} + \mathbf{K}^T \mathbf{S}_y^{-1} \mathbf{K} + \gamma \mathbf{I})^{-1} [\mathbf{K}^T \mathbf{S}_y^{-1} (\mathbf{y} - F(\mathbf{x}_i)) + \mathbf{S}_a^{-1} (\mathbf{x}_i - \mathbf{a})]$$

Equation 2

where \mathbf{K} is the weighting function matrix, which contains the derivatives of the forward model, evaluated at state \mathbf{x}_i . The Levenburg-Marquardt parameter γ controls the rate of convergence towards solution. If $\gamma = 0$ the equation gives the Newtonian method which will directly provide the desired solution, provided the forward model is linear in \mathbf{x} . If this is not the case then a larger value γ can be chosen to reduce the magnitude of the state update. A sufficiently large value for γ should ensure that cost function for \mathbf{x}_{i+1} is smaller than \mathbf{x}_i , as the update will follow the local gradient of the cost function. In the RAL implementation, γ is varied during the iteration process as follows:

- 1) γ is initialised to a "small" (non-zero) value such that initially it has no significant impact on the update of the state-vector. \mathbf{x}_i is initialised to a reasonable first estimate of the state, \mathbf{x}_0 . In this case the *a priori* state is always used as first guess ($\mathbf{x}_0 = \mathbf{a}$).
- 2) \mathbf{x}_{i+1} is evaluated and the cost function value for this state determined.
 - If this cost is larger than that for state \mathbf{x}_i , the update is rejected and γ is increased by a factor of 10. This step is repeated starting from the same \mathbf{x}_i (until a defined maximum number of steps is reached).
 - If the cost is reduced, the update is accepted (\mathbf{x}_i is replaced by \mathbf{x}_{i+1}) and γ is decreased by a factor of 10.
 - If the cost from this iteration has changed by more than 1 (a potentially significant change compared to the defined measurement errors), a new iteration is performed (up to a defined maximum number of iterations).

 UKRI Science and Technology Facilities Council	RAL IASI Methane Retrieval ATBD Version 2.1	2022-07-21
		Page 12 of 42

- Otherwise, convergence is tested by repeating step 2 from the new state estimate with $\gamma = 0$. If again the cost has reduced by less than 1 the retrieval is considered to have converged (and the process finishes).

Assuming the forward model is linear in the relevant range about the solution state and the measurement and *a priori* errors are properly defined, then the error covariance of the solution state is reliably given by

$$\mathbf{S}_x = (\mathbf{S}_a^{-1} + \mathbf{K}^T \mathbf{S}_y^{-1} \mathbf{K})^{-1}$$

Equation 3

The square-roots of the diagonal elements of this matrix give the *estimated standard deviation* (ESD) of each element of the state vector.

The sensitivity of the retrieved state to the true state can also be characterised by the averaging kernel matrix:

$$\mathbf{A} = (\mathbf{S}_a^{-1} + \mathbf{K}^T \mathbf{S}_y^{-1} \mathbf{K})^{-1} \mathbf{K}^T \mathbf{S}_y^{-1} \mathbf{K}$$

Equation 4

Elements of this matrix give the derivatives of each element of the state-vector with respect to changes in its true value (subject to the accuracy of the forward model and its linearisation).

The trace of the averaging kernel (sum of the diagonal elements) gives the number of degrees of freedom for signal (DOFS).

3.4 MEASUREMENTS

3.4.1 IASI

As illustrated in Figure 2, methane is principally observed by IASI in spectral ranges around 1200-1350 cm^{-1} (7.9 μm) in the mid-IR, and 2450-2760 cm^{-1} (3.7 μm) in the short-wave IR (SWIR). Use of the SWIR band is complicated by the fact that the reflected solar contribution is comparable to that thermally emitted by the Earth. However, the solar reflected term in the SWIR can introduce distinct sensitivity to methane near the surface, compared to that which can be obtained from the longer-wave. The potential to use the SWIR range was evaluated in RD-13. So far it has not been possible to make use of this spectral range, partly because of the relative low signal to noise of IASI in the SWIR compared to the TIR range. The RAL methane scheme currently exploits only the TIR spectral range.

Following the work of Razavi et al. (RD-6), we restrict the coverage used in the mid-IR to between 1232.25 and 1290 cm^{-1} . The range above 1290 cm^{-1} is avoided to minimise the impact of neglecting line-mixing on the accuracy of radiative transfer calculations. The range above $\sim 1310 \text{ cm}^{-1}$ is, in any case, of limited use due to the increasingly strong attenuation of the useful signal by water vapour.

Figure 3 shows radiance contributions in the spectral range used in the retrieval. As well as methane, there are significant contributions from water vapour (main isotope), nitrous oxide (N_2O) and the minor water vapour

isotope HDO and methane isotope 13-CH₄. All of these species need to be accounted for in the retrieval. CO₂ and F11 also absorb weakly in the region, but are assumed to be uniformly mixed (and therefore modelled implicitly by RTTOV with fixed profiles).

Within the 1232.25-1290 cm⁻¹ spectral range, the following intervals are omitted due to the presence of relatively strong systematic residuals from non-target species:

- 1245-1246.75 cm⁻¹
- 1267-1270 cm⁻¹
- 1288-1290 cm⁻¹

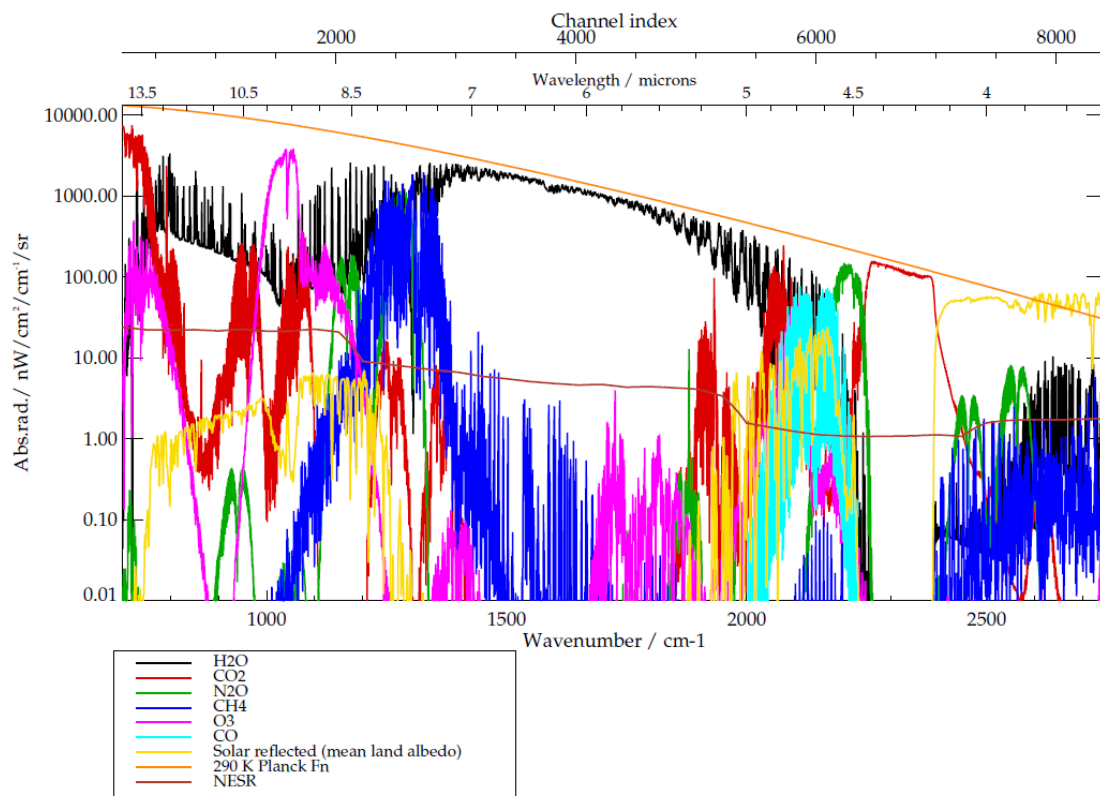


Figure 2: Modelled contributions from dominant absorbers to the total observed IASI radiance (for typical mid-latitude conditions). Yellow line shows for comparison a simply modelled solar reflected radiance (assuming a representative global mean land albedo). The orange line shows the Planck function for a 290 K black body. The brown line shows the nominal IASI NESR.

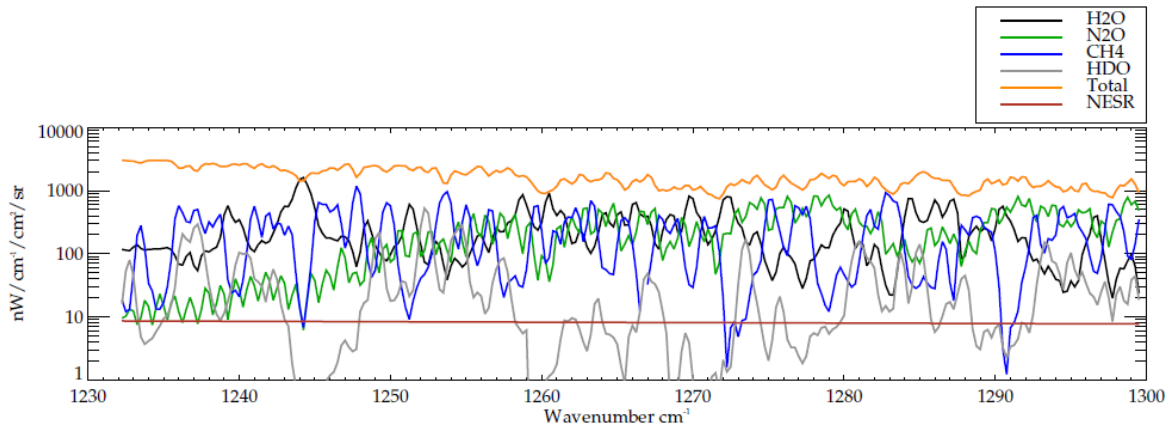


Figure 3: Modelled contributions from dominant absorbers to the total observed IASI radiance (for typical mid-latitude conditions). The orange line shows the modelled radiance including all gases. The brown line shows the nominal IASI NESR.

3.4.2 SELECTION OF IASI OBSERVATIONS

Currently, scenes which are strongly affected by cloud are not processed by the scheme. This selection is made using a brightness temperature difference test to detect optically thick and/or high altitude cloud. The selection checks the difference in brightness temperature between the IASI observation at 950 cm^{-1} and that simulated on the basis of IMS pre-retrieved analysis (the *a priori* state for a standard retrieval as described below). If this difference (observation – simulation) is outside the range of -5 to 15K, retrievals are not processed.

Furthermore, due to the retrieval information content significantly degrading over very cold surfaces and poor convergence when the retrieval is affected by strong near-surface temperature inversions, only scenes with a brightness temperature larger than 240 K at 950 cm^{-1} are processed.

3.4.3 MEASUREMENT ERRORS

Initial retrievals performed by RAL used the NESR for IASI band 2 from the IASI_NCM files provided by Eumetsat. It was found that fit residuals were often considerably better than this noise estimate would predict. It appears that the region of the band which is used is particularly favourable from the point of view of signal to noise. Furthermore, the spectral standard deviation of the fit residuals varies with the scene radiance, in a manner which would suggest signal photon noise to be the main source. The IASI noise is thus modelled (in the fit region) as follows:

$$\Delta y_{noise} = \sqrt{h + o\bar{I}}$$

Equation 5

where

- Δy_{noise} is the estimated standard deviation of the IASI noise in the methane fit range (in $\text{nW}/\text{cm}^2/\text{cm}^{-1}/\text{sr}$), which is assumed spectrally independent. Note that $1\text{ nW}/\text{cm}^2/\text{cm}^{-1}/\text{sr}$ corresponds to $10^{-7}\text{ W}/\text{m}^2/\text{m}^{-1}/\text{sr}$ or (approximately) 0.01 K considering a scene emitting as black body at 280 K.
- h and o are linear fit parameters. In the current retrieval, $o=-26.38$ and $h=0.11067$.

- \bar{I} is the mean observed radiance in IASI band 2 (derived from the L1C spectra, as a proxy for the total input intensity).

In addition, the standard deviation in the agreement between RTTOV and RFM (as shown in Figure 5) is added to this assumed inherent IASI noise, such that the square-root-diagonal elements of the assumed measurement covariance are as follows:

$$\Delta y_i = \sqrt{\Delta y_{noise}^2 + \Delta y_{RTTOV:i}^2}$$

Equation 6

where $\Delta y_{RTTOV:i}$ is the standard deviation in the difference between RTTOV and IASI in channel i .

The measurement covariance is assumed to be diagonal.

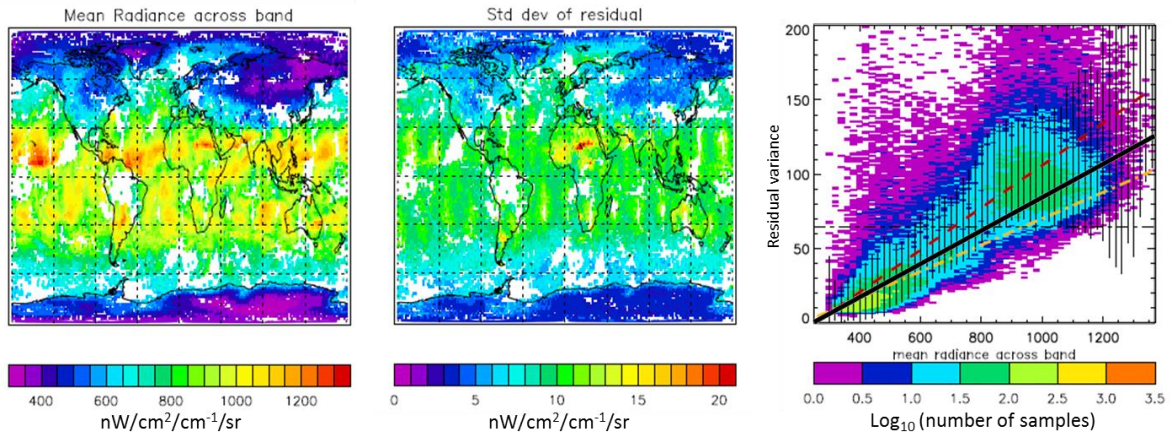


Figure 4: Derivation of noise model. Left-hand panel shows the mean IASI radiance across band 2. Centre panel shows the spectral standard deviation of actual fit residuals. Right-hand panel shows the scatter density of the points on the map. Results are taken from a single day of observations. The black line shows the simple linear noise model currently assumed. Dashed horizontal line shows the nominal IASI noise (from IASI_NCM files) in the methane fit window.

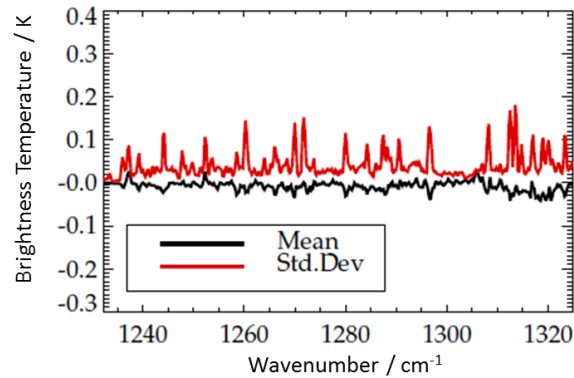


Figure 5: Mean and standard deviation in the brightness temperature differences between RTTOV (with RAL coefficients) and RFM line-by-line model.

3.5 FORWARD MODEL

The forward model (FM) used in the RAL IASI CH₄ OE Retrieval is RTTOV (currently version 10.2). RTTOV estimates radiances convolved with the IASI spectral response function by use of spectrally-averaged layer transmittances, based on a fixed set of coefficients which weight atmospheric-state-dependent predictors. The model is sufficiently fast to enable global processing of the IASI mission with modest computational resources.


RTTOV parameterises the instrument resolution transmission from space to a given atmospheric layer using coefficients derived using a line-by-line (LBL) radiative-transfer model. In order to allow HDO and 13-CH₄ to be modelled as a variable species, coefficients for RTTOV have been specifically determined for the relevant spectral range by RAL. These are based on running the Oxford Reference Forward Model, RFM (ER-1), using HITRAN 2008 (RD-5) (assuming no line-mixing). Calculations are performed for the same set of atmospheric profiles used to obtain the standard RTTOV coefficients for IASI (as described in RD-22). (The predictors which are regressed against these LBL calculations are also identical to those used in the standard RTTOV code).

In order to include HDO, without the need to change the RTTOV code itself (only the coefficients), HDO is modelled using the RTTOV variable that nominally represents carbon monoxide (CO) and 13-CH₄ is modelled using the ozone (O₃) profile. Thus, the CO and ozone predictors are used to represent the transmission differences introduced by HDO and 13-CH₄, respectively, as independent, variable species. More details on the RAL approach to deriving RTTOV coefficients is provided in RD-8.

3.6 STATE VECTOR

The state vector for the retrieval scheme consists of 35 elements, as follows:

- Surface temperature (K).
 - *a priori* value: from pre-retrieved IMS data (see section 3.6.1 below).
 - *a priori* error: 5K

 UKRI Science and Technology Facilities Council	RAL IASI Methane Retrieval ATBD Version 2.1	2022-07-21
		Page 17 of 42

- Methane mixing ratio (ppmv) defined on 12 fixed pressure levels corresponding to z^* values of 0, 6, 12, 16, 20, 24, 28, 32, 36, 40, 50, 60 km, where z^* is a simple transformation of pressure, p , (in hPa) to approximate geometric altitude (km):

$$z^* = 16 (3 - \log_{10}(p))$$

Equation 7

The *a priori* profiles for methane are defined in a deliberately simple manner to ensure that variations in the resulting products are clearly driven by measurement information. The approach is described in section 3.6.3 below. Note that the FM linearly interpolates the state vector representation of the profile (vmr as function of z^*) onto the much more finely resolved RTTOV internal pressure grid ¹.

- Natural logarithm of the water vapour (H₂O) mixing ratio (ppmv) defined on 16 fixed pressure levels corresponding to z^* values of 0, 1, 2, 3, 4, 5, 6, 8, 10, 12, 16, 20, 30, 40, 50, 60 km. The *a priori* profiles for water vapour are taken from IMS analysis, interpolated (linearly) onto these pressure levels.
- Scale factor for HDO. The HDO mixing ratio profile, $r_{HDO}(p)$ is assumed to be given by


$$r_{HDO}(p) = f_{HDO} f_{iso} r_{H2O}(p)$$

Equation 8

where f_{HDO} is the retrieved HDO scale factor; f_{iso} is (fixed) isotopic ratio of HDO compared to the main water vapour isotope assumed by HITRAN (3.107×10^{-4}) and $r_{H2O}(p)$ is the (retrieved) water vapour main isotope mixing ratio profile.

- *A priori* value: 1
- *A priori* error: 1
- Scale factor for the ratio of 13-CH₄ to the main methane isotope (defined in same way as the HDO isotope factor, with same *a priori* value and error).
- Natural logarithm of the cloud fraction, where cloud is modelled in RTTOV as a black body at a specific altitude occupying a defined horizontal geometric fraction of the modelled scene.
 - *A priori* value: -2.303 (corresponding to absolute cloud fraction of 0.01 when converted from the logarithmic representation in the state vector)
 - *A priori* error: 10 (specifying a fractional variation by factor 10 from the 0.01 *a priori* value)
- Cloud pressure (as above).
 - *A priori* value: 500 hPa
 - *A priori* error: 500 hPa
- Scale factor for mean fit residual (see section 3.8)
 - *A priori* value: 1
 - *A priori* error: 1
- Scale factor for across-track fit residual (see section 3.8)
 - *A priori* value: 0

¹ It is important to reproduce this assumption when computing vertically integrated quantities from the retrieved profile.

 UKRI Science and Technology Facilities Council	RAL IASI Methane Retrieval ATBD Version 2.1	2022-07-21
		Page 18 of 42

- *A priori* error: 1

As noted above, the logarithm of the physical value is adopted for some elements of the state vector. This is done to prevent the corresponding physical values from becoming negative leading to non-physical solutions.

Note that the profiles in the state vector are always defined on the fixed levels, even if these are below the surface pressure. Profiles are always interpolated (linearly in log pressure) onto the fixed 101 pressure levels on which the RTTOV coefficients are defined before being input to RTTOV. The surface pressure (from IMS) is also passed to RTTOV. Profile values below the surface pressure are ignored by RTTOV. Retrieved profiles (and the associated error characterisation) should be interpreted with this in mind – for example, the column averaged mixing ratio should be determined by reproducing the interpolation onto RTTOV levels and integrating from the surface pressure to space.

3.6.1 USE OF IMS DATA

The RAL Infrared Microwave Sounding (IMS) scheme developed during the study “Optimal Estimation Method retrievals with IASI, AMSU and MHS measurements” [RD-15] enhances the 1DVar optimal estimation aspect of the EUMETSAT IASI L2 retrieval and is explained in detail in RD-15.

The IMS scheme uses data from IASI and both microwave (MW) instruments on-board the MetOp platform; the Microwave Humidity Sounder (MHS) and the Advance Microwave Sounding Unit (AMSU). Inclusion of the MHS and AMSU MW channels allows temperature and water vapour soundings of the lower atmosphere even in the presence of some cloud.


The IMS state vector is expressed in terms of Principle Component (PC) weights with 28 for the atmospheric temperature profile, 18 for the humidity profile, 10 for the ozone profile and 20 for the spectral emissivity. The state vector also includes elements for surface temperature, a spectral radiance bias correction factor (BCF), cloud-top height (CTH), cloud fraction (CF) and cloud ice fraction (CIF).

Climatological monthly zonal mean profiles are used as the prior state for temperature humidity and ozone. The profile principal components (and *a priori* errors) represent the variability of ECMWF profiles about the climatological zonal mean.

In the retrieval of spectral emissivity, PCs were computed from the global covariance of the RTTOV implementation of the UW IR spectral emissivity database [RD-4, ER-3] and RTTOV MW spectral emissivity models. Spectral correlations between the IR and MW emissivities are included (derived from the RTTOV representation of the spatial covariance of IR and MW emissivity).

Retrievals make use of pre-retrieved IMS data to define the following:

- Atmospheric temperature profile.
- *A priori* value of the surface temperature.
- The *a priori* water vapour profile.
- Land surface spectral emissivity. IMS provides emissivity in the sub-set of 139 IASI channels that it fits. The spectral emissivity used in the methane retrieval is given by the linear interpolation of the emissivity at IMS channels in the fit range (1230, 1234.25, 1239.25, 1240.5, 1242.75, 1244.25, 1245.25,

 UKRI Science and Technology Facilities Council	RAL IASI Methane Retrieval ATBD Version 2.1	2022-07-21
		Page 19 of 42

1247.5, 1252, 1257.75, 1260.25, 1266.25, 1268.25, 1271, 1278.5, 1282.5, 1284, 1285.5, 1288.75, 1291, 1293, 1293.5, 1296.75, 1300 cm⁻¹).

3.6.2 USE OF ECMWF DATA

Retrievals make use of ECMWF data to define the following:

- Surface pressure.
- Potential vorticity, which in turn defines equivalent latitude and the assumed N₂O field (see below).
- Wind speed for the sea emissivity model in RTTOV.

Currently ERA-5 data is used, taken from the Centre for Environmental Data Analysis (CEDA). The form of ERA interim output available at the CEDA has the following characteristics:

- Horizontal resolution: 0.25° (latitude and longitude)
- Vertical resolution: 137 model levels from surface ~0.01 hPa
- Temporal resolution: hourly analysis.

For use in retrievals, EMCWF data is obtained at the nearest hour to a given observation. The field is bi-linearly interpolated in latitude and longitude to the location of a given IASI observation.

3.6.3 METHANE A PRIORI

The methane *a priori* profiles are based on a combination of TOMCAT (ER-22) and MACC greenhouse gas flux inversion fields.

TOMCAT output based on the stratospheric assimilation (RD-9) of measurements by the ACE-FTS instrument was provided by the University of Leeds. These cover the period from 14 September 2008 to 9 September 2010, sampled every 6 hours at a horizontal resolution of approximately 2.8 degrees, with 60 vertical levels from the surface to 0.1 hPa. The zonal, annual mean of this dataset is determined using 5 degree latitude bins, interpolating profiles from the model levels onto a set of 65 fixed pressure levels (z^* values of 0 to 64 km in 1 km intervals). The corresponding standard deviations in the zonal mean are also determined (shown in the left hand panels of Figure 6). This is used to define the stratospheric distribution.

In the troposphere, a fixed vertical profile is assumed with latitude dependence taken from the annual zonal mean lower tropospheric mixing ratio of methane from the MACC greenhouse gas flux inversion data for 2009 (“v10-S1NOAA_ra”, see RD-20). For this purpose the tropopause is assumed to correspond to the methane mixing ratio contour of 1.6 ppmv. The zonal mean methane values 3 km (in z^* units) below this contour are set to that from the annual zonal mean MACC flux inversion. Linear interpolation is then used up to the 1.6 ppmv contour. The resulting mean methane field is shown in the left hand panel of Figure 6.

The *a priori* profile and errors used for a specific IASI retrieval are derived from these annual mean and TOMCAT standard deviations as follows:

1. To avoid strong and very height-dependent constraint to the *a priori*, a minimum, relative error of 10% is imposed for the assumed prior errors. This is imposed in root-sum-square fashion as follows:

$$\Delta x_{ij} = \sqrt{\Delta x_{T:ij}^2 + (0.1 x_{T:ij})^2}$$

Equation 9

where Δx_{ij} is the adjusted standard deviation for latitude bin i and pressure level j ; $\Delta x_{T:ij}$ is the corresponding original TOMCAT derived standard deviation and $x_{T:ij}$ is the TOMCAT/MACC derived mean value. The adjusted standard deviations are shown in the right hand panel of Figure 6.

- The methane *a priori* profile and error is obtained by linearly interpolating the adjusted mean and standard-deviation fields to the latitude of the IASI observation, using the centre latitudes of each 5° zonal grid box. The values are also interpolated in altitude to the pressure levels defined in section 3.6.

Diagonal elements of the *a priori* covariance are set to the square of the adjusted standard deviations. Off diagonal elements are defined assuming a Gaussian correlation in the vertical with full-width half-maximum 6 km (in z^* units).

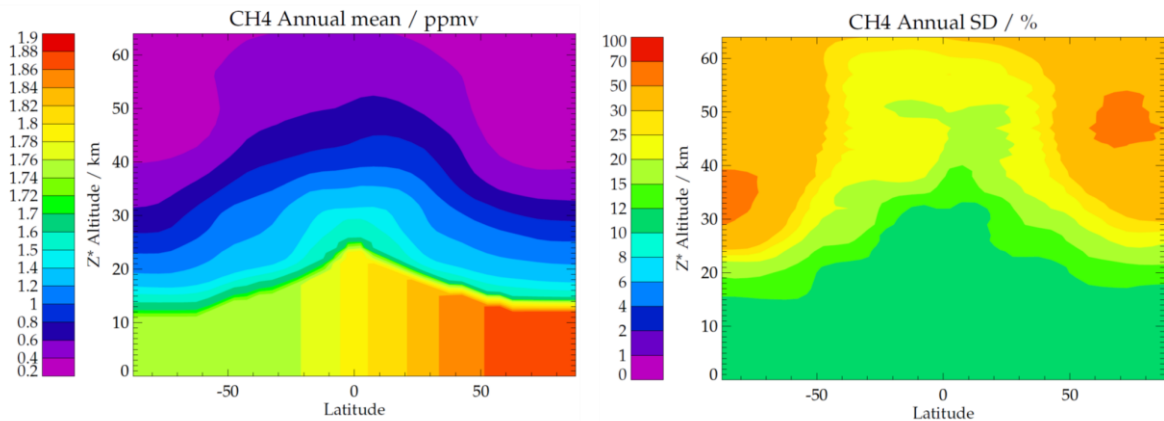


Figure 6: Illustration of methane *a priori* profiles and errors, derived from the TOMCAT and MACC fields. Left-hand panel shows 5 degree multi-annual zonal mean, used as the *a priori* profile. Right-hand panel shows the assumed standard deviation (SD), used as the *a priori* error.

3.6.4 WATER VAPOUR

The *a priori* water vapour was originally (in the v1.0 scheme) taken from ECMWF analysis. In the version 2.0 scheme the *a priori* state is taken from the IMS output, however the same *a priori* covariance as the v1.0 scheme is used. This is defined to account for errors in the analysis, including those introduced by the relatively low spatial and temporal resolution of the available ERA-interim data. Although these errors are not strictly representative of errors in IMS retrievals, the covariance is still found to be suitable for methane retrieval purposes. It is defined as follows:

ERA interim data is taken for all four of the 6 hourly analysis times on a single day. The global covariances of differences between neighbouring times and between neighbouring spatial samples (shifting one grid point in both latitude and longitude dimensions) are determined:

$$C_{space:ij} = \frac{1}{N_{lat}N_{lon}N_t} \sum_{klm} (x_{i,k+1,l+1,m} - x_{i,k,l,m})(x_{j,k+1,l+1,m} - x_{j,k,l,m})$$

Equation 10

$$C_{time:ij} = \frac{1}{N_{lat}N_{lon}N_t} \sum_{klm} (x_{i,k,l,m+1} - x_{i,k,l,m})(x_{j,k,l,m+1} - x_{j,k,l,m})$$

Equation 11

where

- $x_{i,k,l,m}$ is the water vapour mixing ratio at model level i , latitude k , longitude l and time m .
- N_{lat} (=256) is the number of latitude grid points (corresponding to index k).
- N_{lon} (=512) is the number of longitude grid points (corresponding to index l).
- N_t (=4) is the number of time samples (corresponding to index m).

Also considered is the ECMWF forecast background covariance (provided by ECMWF in 2010, considered representative of the GEMS/MACC systems). A single covariance is provided, considered to be representative globally.

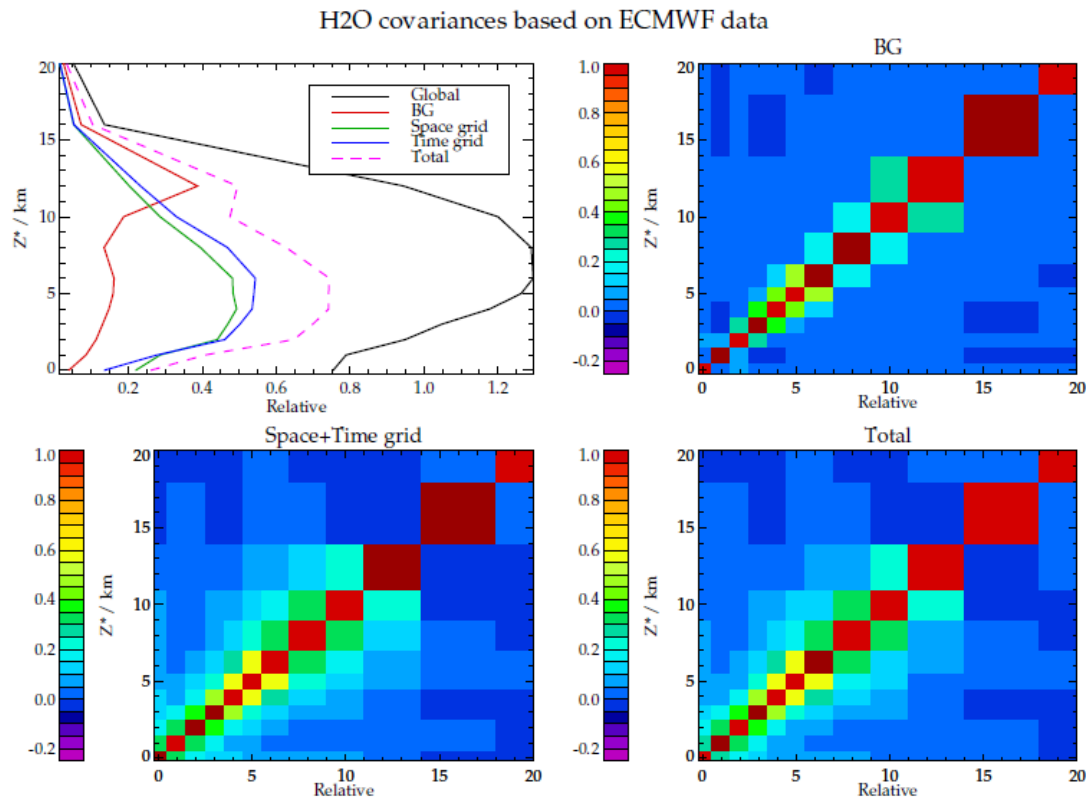



Figure 7: Illustration of water vapour error covariances. The “total” error covariance is used as the prior covariance for water vapour in the retrieval. In the top left hand panel, coloured lines show standard deviations (relative to the mean profile) of the various covariance

 UKRI Science and Technology Facilities Council RAL Space	RAL IASI Methane Retrieval ATBD Version 2.1	2022-07-21
		Page 22 of 42

matrices described in the main text. The black line shows the global standard deviation of water vapour from the mean value (for reference only).

The covariances are projected onto the retrieval grid as follows:

1. The eigenvectors (principal components) and eigenvalues of the covariance (on the model grid) are obtained such that

$$C = U^t \Lambda U$$

Equation 12

where

- C is the original covariance matrix of eigenvectors
 - U is the matrix of eigenvectors of C
 - Λ is the diagonal matrix containing the corresponding Eigenvalues.
2. The eigenvectors are interpolated onto the retrieval grid, using the pressure profile of the model grid, when surface pressure is 1013.25 hPa.
 3. The covariance is reconstructed from the interpolated Eigenvectors (same Eigenvalues):

$$C' = U'^t \Lambda U'$$


Equation 13

The retrieval uses the total of the covariance associated with spatial and temporal shifts and the defined background covariance. These are illustrated in Figure 7. Note that the space and time covariances are comparable, and both generally larger than the background covariance, except in the upper troposphere. The total covariance has standard deviation about half of that of the global variation of water vapour from the global mean profile (see black line in the top-left panel of Figure 7).

3.7 MODELLING N₂O

A fundamental feature of the RAL scheme is realistic modelling of the N₂O profile such that the associated absorption features can be exploited to enable cloud impacts on the methane retrieval to be accommodated via retrieved effective cloud fraction and height. N₂O is extremely well mixed in the troposphere and while the tropospheric distribution of N₂O is less variable than methane, N₂O has a stronger gradient above the tropopause. This leads to the influence of the stratosphere on the total column being greater. It is therefore important to accurately model the N₂O profile shape at the location of individual IASI observations. In this scheme, variations in N₂O in the stratosphere are modelled assuming the photochemically-induced variations are captured by a monthly zonal mean climatology and that the dynamically-induced variations can be modelled using equivalent latitude (RD-10, RD-11), derived from ECMWF analysed vorticity.

Because the photochemical processes controlling stratospheric N₂O have relatively long time-scales compared to that of horizontal transport, there is an extremely strong, compact correlation between potential vorticity (PV) and the mixing ratio of N₂O, on a given potential temperature surface. Exploiting this relationship, the climatological N₂O distribution can be conveniently expressed in terms of equivalent latitude, which is effectively a (isentropic level specific) unit conversion of PV: equivalent latitude is defined as the latitude circle that encloses the same poleward area as a given PV contour, on surfaces of constant potential temperature.

 UKRI Science and Technology Facilities Council RAL Space	RAL IASI Methane Retrieval ATBD Version 2.1	2022-07-21
		Page 23 of 42

For current retrievals, the ACE-FTS seasonal climatology for N₂O (RD-12) is used, which is provided directly as a function of equivalent latitude. This is filled below the tropopause with a fixed mixing ratio of 322 ppbv. This climatology is linearly interpolated in day of year to the date of a given IASI observation. The 3D (latitude, longitude, height) distribution corresponding to a given ECMWF analysis time is inferred from this 2D (equivalent latitude, potential temperature) distribution as follows:

1. ECMWF analysed vorticity fields on model levels are converted to potential vorticity on potential temperature levels using standard routines provided by the Met Office. A fixed set of potential temperature levels which oversample the standard model vertical grid by a factor of 2 is used to avoid undersampling the model structure.
2. A set of PV values are defined for each level. The equivalent latitude corresponding to each of these PV values (on each level) is evaluated, by computing the poleward area occupied by grid boxes with PV greater than the each given value. This gives a look-up-table (LUT) for each level that translates PV values to equivalent latitude.
3. The LUT is linearly-interpolated to the PV at all ECMWF model grid points, to give the equivalent latitude distribution on the ECMWF horizontal grid.
4. The horizontally-gridded equivalent latitudes are interpolated vertically to the original model vertical grid. This provides fields of equivalent latitude on the same grid as other ECMWF profile variables (temperature, humidity). The corresponding N₂O distribution is derived by bi-linearly interpolating the equivalent latitude / potential temperature climatology.
5. The resulting “equivalent N₂O” field is then interpolated to the IASI measurement location and time in the same way as other profile variables (see section 3.6.2).

It is assumed that N₂O is increasing linearly with time at a rate of 0.23% / year. This is currently achieved by multiplying the N₂O field as derived above (at all altitudes) by the factor:

$$f = 1 + \frac{0.0023}{365.25} d$$

Equation 14

Where d is the number of elapsed days since the beginning of 2009. From validation conducted in previous studies (RD-14), this approach seems appropriate at least until the end of 2013. This growth rate was derived from observed trends in flask data at Mauna Loa (from the NOAA Global Monitoring Laboratory, ER4). It may be desirable to improve this approach e.g. using more detailed modelling in combination with surface observations of N₂O.

It is noted that the retrieved methane responds quite linearly to perturbations in the modelled N₂O column (a given relative perturbation in N₂O will translate into a similar relative perturbation in methane). It is therefore possible to approximately correct retrievals if better information on the N₂O column is available post hoc.

3.8 FITTING OF SYSTEMATIC RESIDUAL PATTERNS

If no correction is applied, the retrieval is found to have small but significant systematic fit residuals, which vary with across-track scan angle (<0.5 K in brightness temperature). The scheme would also produce methane mixing ratios which are generally positively biased compared to other data (TCCON, GOSAT, state of the art models). In order to reduce these effects, the following procedure is adopted:

1. In the latitude range of 75° S to 15° S, the methane mixing ratio is fixed to “equivalent” CH₄ profiles defined in the same way as that described for N₂O, above. The profiles are scaled such that the average fit residual for the nadir observations (i.e. across-track scan index 15 out of the 30 across track positions) is negligibly correlated with the weighting function for a scaling of the methane profile.
2. From these retrievals we derive the (i) the mean fit residual from the nadir retrieval (all 4 detectors of scan index 15) , r_0 ; (ii) the mean residual considering both outer edges of the swath (all 4 detectors in scan indices 1 and 30) , r_E . The difference between these two patterns is also determined, $r_1 = r_E - r_0$. Patterns r_0 and r_1 are illustrated in Figure 8.
3. In the standard retrieval, patterns r_0 and r_1 are added to the simulated observations, after each being multiplied by a retrieved scaling factor (f_0 and f_{01} , respectively). That is, the simulated measurement used in the retrieval is given by

$$y' = y_{RTTOV} + f_0 r_0 + f_1 r_1$$

Equation 15

where y_{RTTOV} is the result from RTTOV, for the current estimated state.

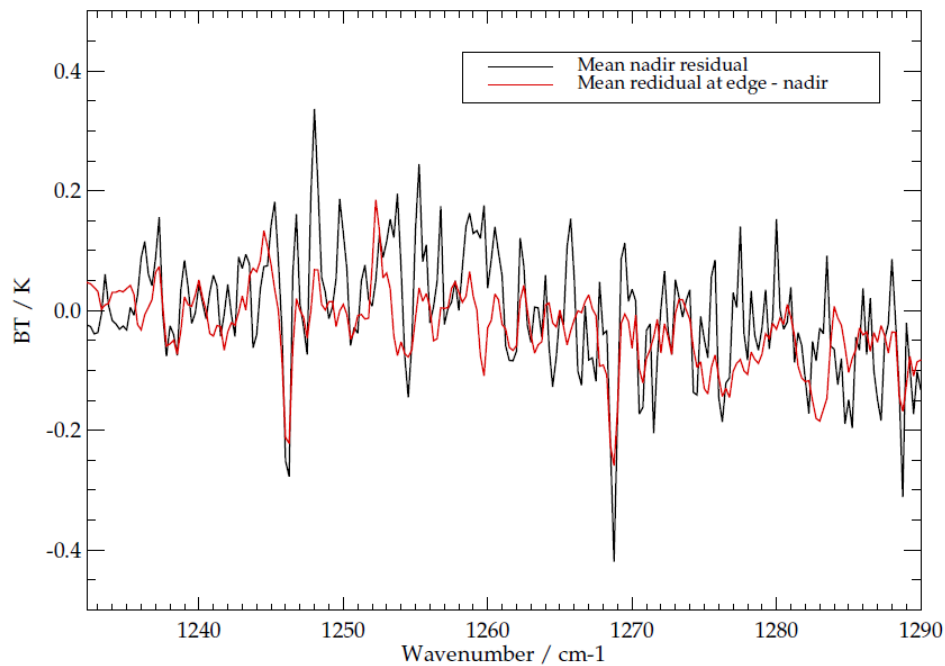



Figure 8: Systematic residual patterns used in the current retrieval (derived from measurements on 28 August 2009). Black line shows the mean residual for nadir observations, i.e. index 15 of the 30 across-track views, averaged over all four detectors. Red line shows the difference between mean of the residual for both extreme scan position (index 1 and 30) and the mean nadir residual.

 UKRI Science and Technology Facilities Council	RAL IASI Methane Retrieval ATBD Version 2.1	2022-07-21
		Page 25 of 42

4 RETRIEVAL SCHEME CHARACTERISATION AND ERROR ANALYSIS

Here we present an overview of the retrieval characterisation by summarising the OEM retrieval diagnostics provided by the scheme. Validation results are provided elsewhere (RD-14, RD-16).

Although the retrieval directly fits the methane profile, height-resolved information is limited and it is usually more useful to consider vertically integrated quantities, derived from the profile. Here we consider mainly the total column average mixing ratio and sub-column averages between the lower retrieval levels, in particular the “0-6 km” and “6-12 km” sub-columns, where the pressure-altitudes are in z^* (Equation 7), and 0 refers to the Earth’s surface. Dry air (sub-) column average mixing ratio is the vertically integrated number of molecules of methane (per unit surface area) divided by the similarly vertically integrated number of air molecules (excluding water vapour).

The transformation from the retrieved methane mixing ratio profile, \mathbf{x} , to the dry-air column averaged mole fraction, c , can be expressed as a matrix operation $c = \mathbf{M}\mathbf{x}$, where \mathbf{M} contains the weights required to perform the linear operations to (i) interpolate the profile defined on the state vector grid to the finer grid used in the radiative transfer model (ii) integrate to give the total column amount (iii) normalise by the total column of dry air. The ESD of the column average is then given by:

$$\Delta c = \sqrt{\mathbf{M} \mathbf{S}_x \mathbf{M}^T}$$

Equation 16

The sensitivity of the retrieval to perturbations in the measurement is given by the gain matrix, $\mathbf{G} = \mathbf{S}_x \mathbf{K}^T \mathbf{S}_y^{-1}$. The sensitivity of the retrieval to perturbations in the true state vector is characterised by the averaging kernel, $\mathbf{A} = \mathbf{G}\mathbf{K}$.

Issues relating to the sensitivity of the retrieval to vertical structure and smoothing errors can be addressed using the fine-scale averaging kernel:

$$\mathbf{A}_f = \mathbf{G}\mathbf{K}_f$$

Equation 17

The weighting function \mathbf{K}_f is distinguished from \mathbf{K} in that derivatives may be computed with respect to perturbations on a finer grid than that used for the state vector. The averaging kernel for the sub-column average is $\mathbf{A}_{cf} = \mathbf{M}\mathbf{A}_f$.

The sensitivity of the retrieval is dependent on meteorological conditions (particularly the surface/atmospheric temperature profile and thermal contrast between atmosphere and surface). This is reflected in the geographical and seasonal variation in the profile ESDs as summarised, using retrieval results in 2009 and 2010, in Figure 9. Corresponding errors for the total column are shown in Figure 10 (for zonal means) and Figure 11 (as maps). Errors in the total column average are much smaller than at any individual retrieval level, because profile errors for neighbouring levels are anti-correlated. Values shown are averages over all IASI retrievals for January and July 2009, in 10 degree latitude bands. In the figure, the two months are presented as *winter* and *summer* conditions, with data for summer conditions taken from the January zonal mean in the southern hemisphere and the July mean in the north (vice-verse for the winter). Figure 12 to Figure 14 show the averaging kernels for the total, 0-6 km and 6-12 km columns, respectively. These are shown as a function of altitude but

normalised such that they represent the expected perturbation in the given absolute column amount (in molecules per cm^2) with respect to a delta function perturbation in the same unit at a given altitude. I.e. under ideal circumstances, the total column kernel would be 1 at all altitudes; the 0-6 km sub-column kernel would ideally be 1 between 0 and 6 km, and zero above.

Diurnal variations in surface temperature and air-ground thermal contrast cause the sensitivity of methane retrievals over land to differ between daytime (descending node, 9:30 am local solar time) and night-time (ascending node, 9:30 pm) observations. Methane retrievals over land generally show greater near-surface sensitivity in daytime than night-time. Due to thermal inertia of the ocean, methane retrieval performance is more uniform with respect to latitude, season and time of day than it is over land, however vertical sensitivity can be complicated where warm air from the land is blown over a colder sea surface. This effect leads to some increases in total column ESD to the west of continents in Figure 11. In summer, daytime sensitivity is greater over land than sea; however, the situation is reversed in the winter at mid-latitudes (when the sea is typically warmer than the land).

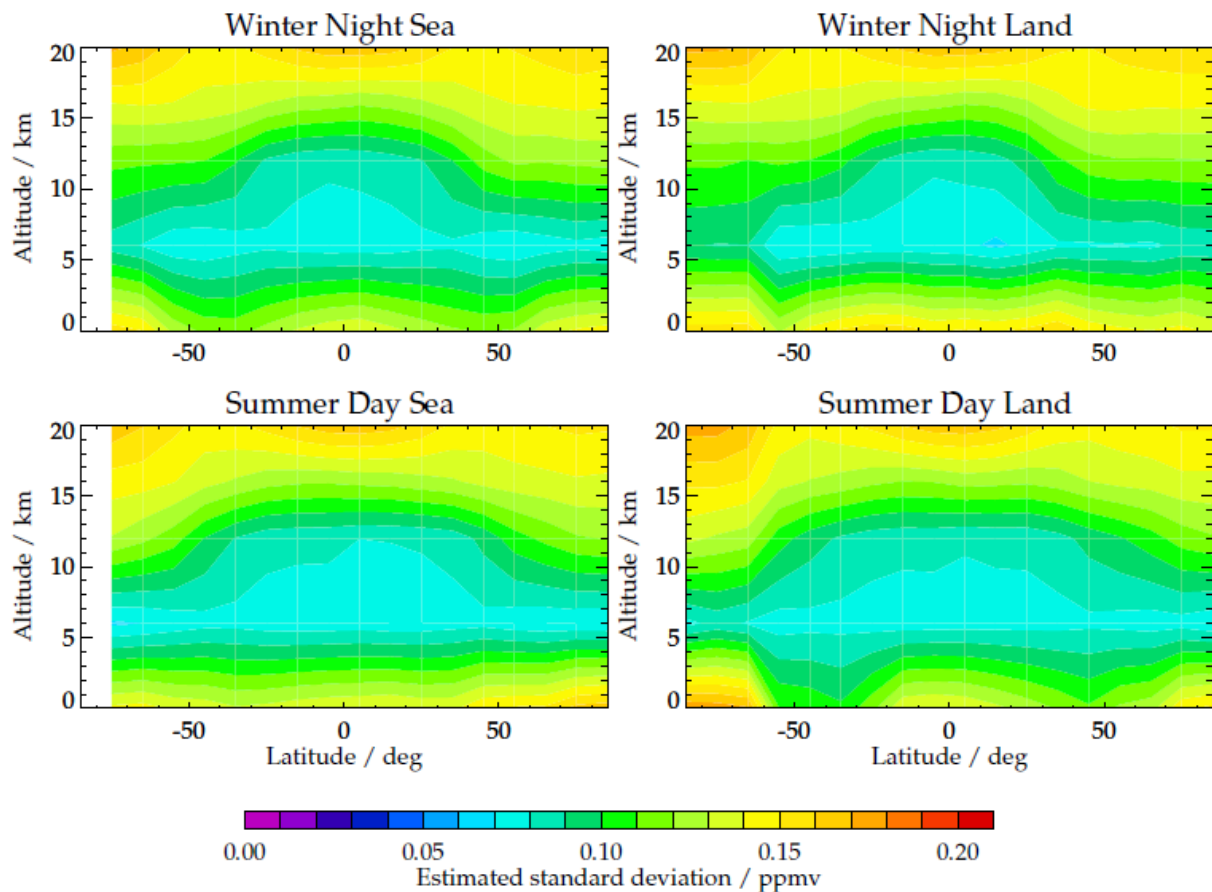


Figure 9: Estimated standard deviation of the methane profile as a function of latitude and season, for observations in winter night and summer daytime over land and sea.

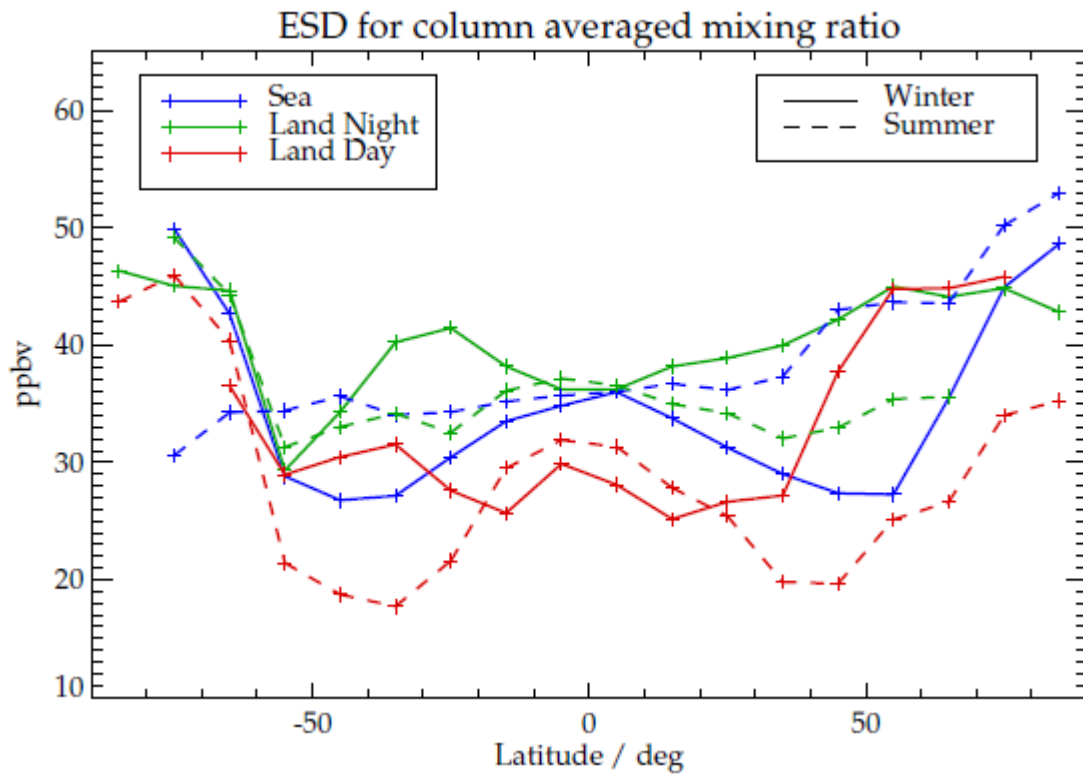


Figure 10: Estimated standard deviation of retrieval total column averaged methane as a function of latitude and season, for observations over sea, daytime land and night-time land.

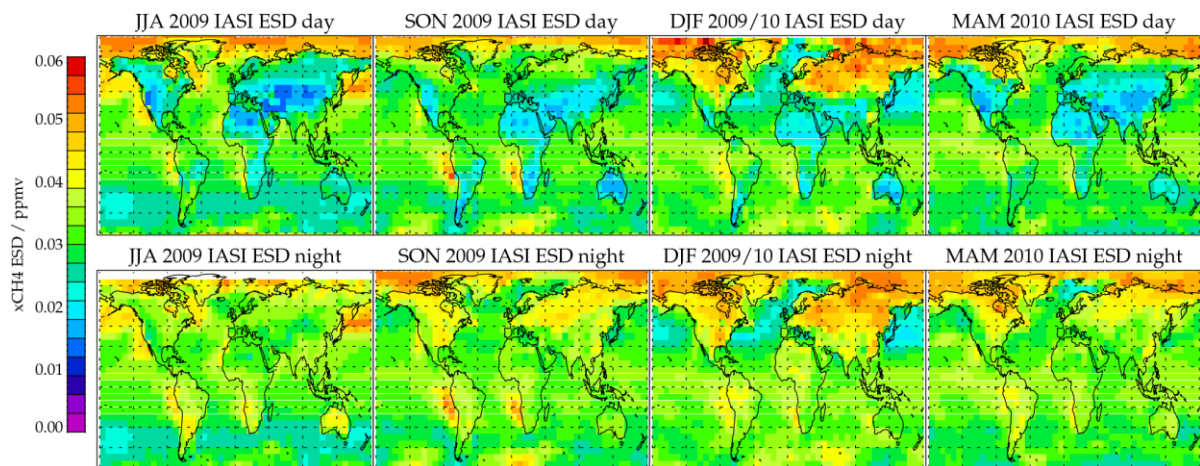
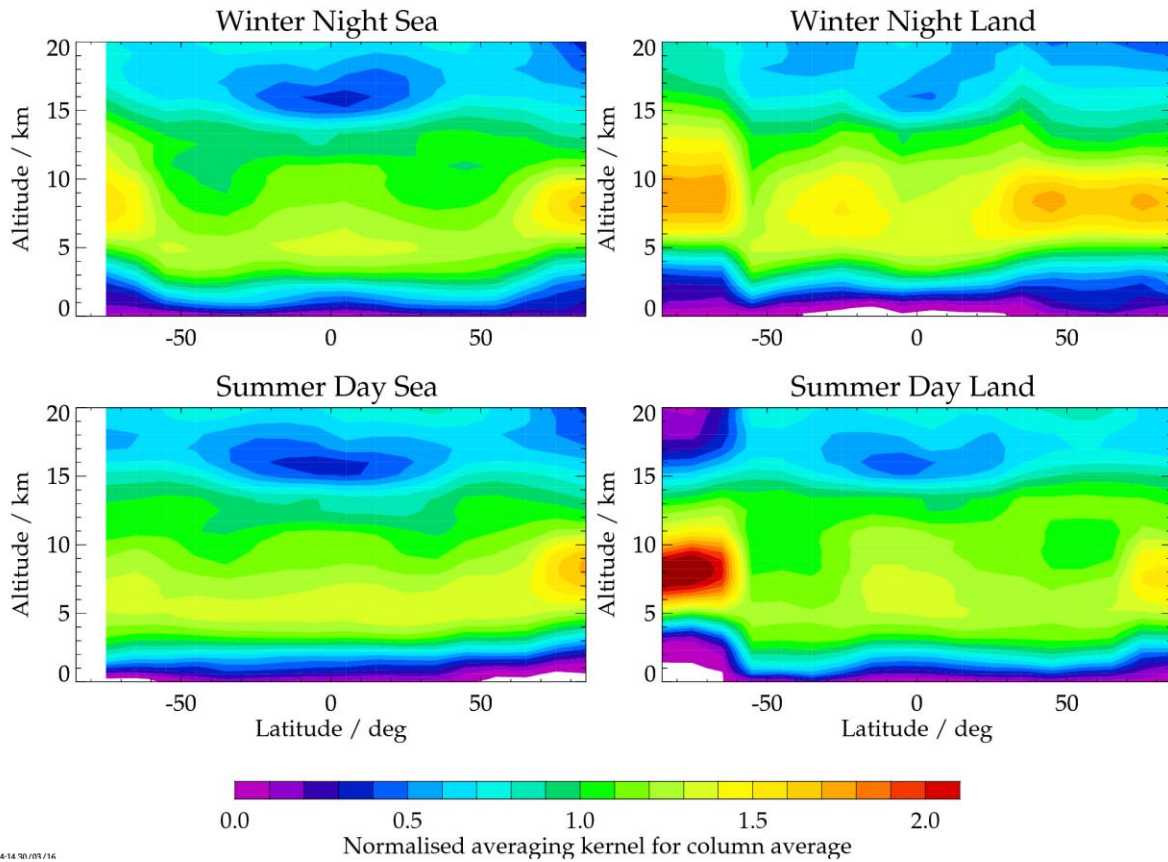


Figure 11: Average in 7.5 x 5 degree latitude/longitude bins of the ESD on the column average mixing ratio as a function of season (left to right) and for day (top) and night-time observing conditions (bottom row). "JJA" = June, July August 2009; "SON" = September, October November 2009; "DJF" = December, January, February 2009/10; "MAM" = March, April, May 2010.



14-14-20/03/16

Figure 12: Averaging kernels for column averaged methane as a function of latitude and season, for observations in winter night and summer daytime over land and sea.

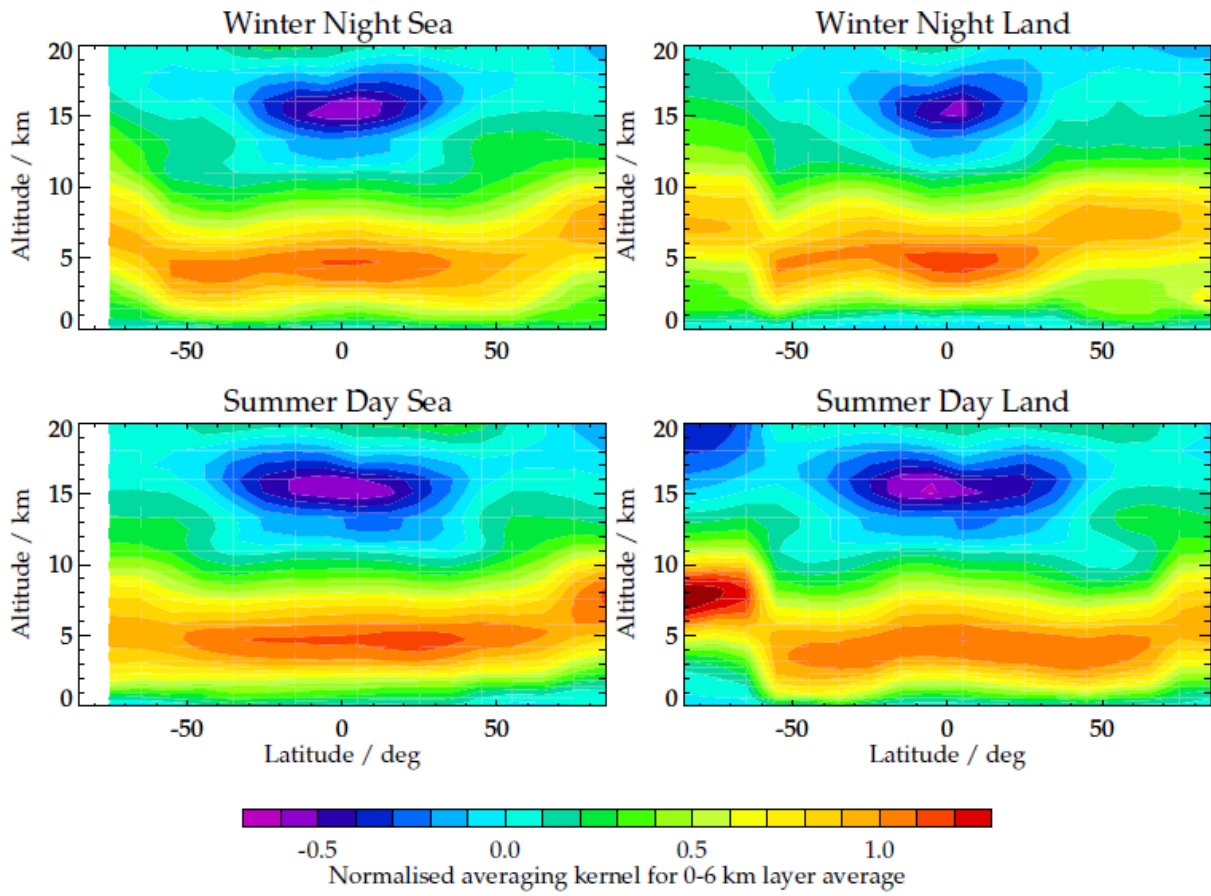


Figure 13: Averaging kernels for 0-6 km sub-column averaged methane as a function of latitude and season, for observations in winter night and summer daytime over land and sea.

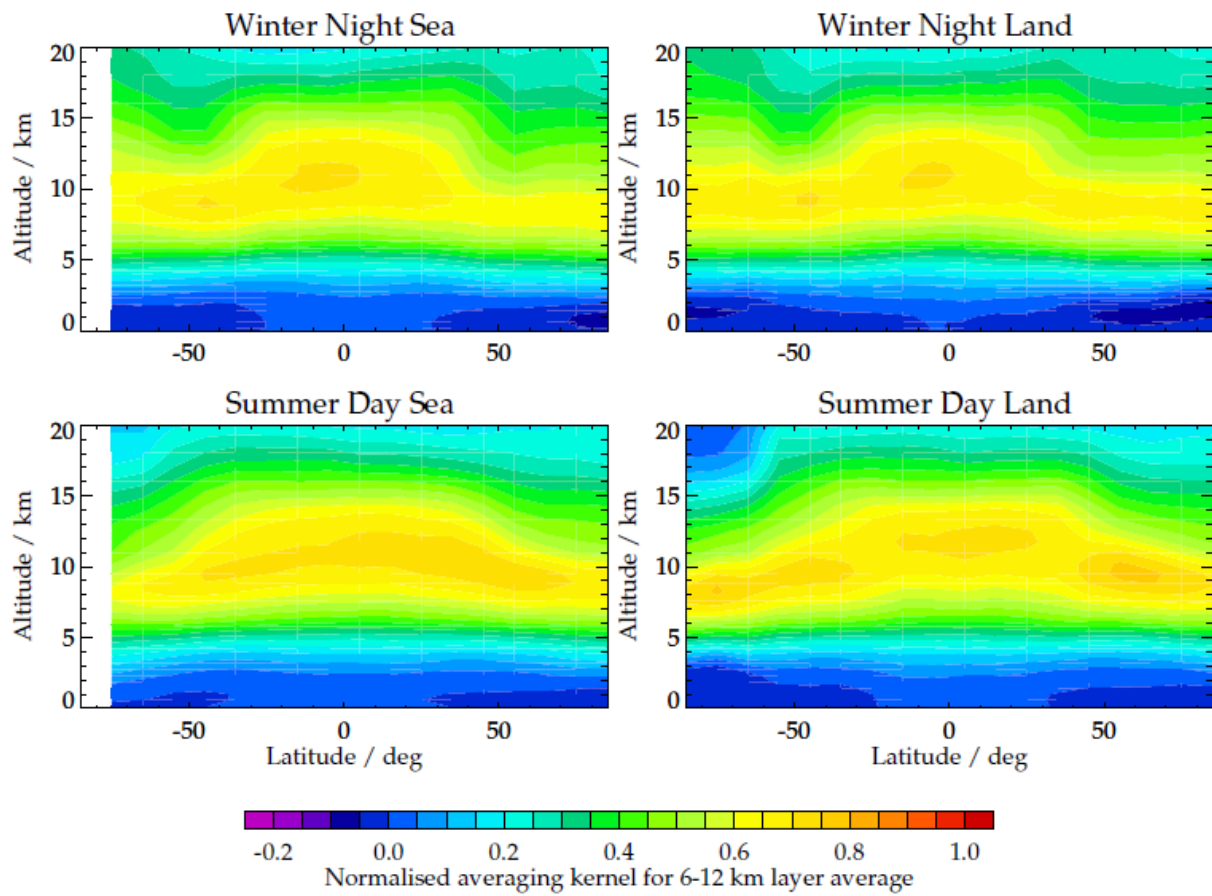



Figure 14: Averaging kernels for 6-12 km sub-column averaged methane as a function of latitude and season, for observations over sea, daytime land and night-time land.

 UKRI Science and Technology Facilities Council	RAL IASI Methane Retrieval ATBD Version 2.1	2022-07-21
		Page 31 of 42

5 CANDIDATE V3 ALGORITHM

5.1 OVERVIEW


During the ESA Methane+ project, a number of potential algorithm improvements were considered leading to the definition of a RAL “candidate v3” algorithm. This was used in the project to generate a “Methane+ version 2” dataset. The differences between this updated algorithm and the version 2 scheme described above are summarised here.

5.2 USE OF IMS DATA

The IMS data (used for temperature profile and surface emissivity) is now taken from the latest version of the IMS scheme, referred to as the “IMS-extended” scheme. IMS-extended exploits new capabilities of RTTOV12 as follows:


- Cloud and aerosol (dust + volcanic sulfuric acid aerosol) are modelled as scattering profiles using realistic optical properties². IMS retrieves the following cloud / aerosol parameters:
 - Water cloud height, optical depth and effective radius. The cloud phase (ice or liquid) is defined using standard brightness temperature difference flags in the 10-12 micron window region. Cloud is assumed defined as an extinction coefficient profile, with Gaussian shape with 1km full-width-half-maximum (FWHM), peaking at the retrieved cloud height.
 - Height and optical depth of desert dust aerosol, again assuming a 1km FWHM Gaussian extinction coefficient profile shape.
 - Optical depth of sulfuric acid aerosol, assuming this to be at ~20km height and have a 2km FWHM Gaussian profile shape.
- Total column amounts of several minor gases are fitted, including SO₂ (sulfur dioxide), CH₃OH (methanol), NH₃ (ammonia), HNO₃ (nitric acid), HCOOH (formic acid).
- The number of IASI channels used is increased, mainly to improve the information content on ozone.
- Ice-free land surface reflectance is modelled as Lambertian, instead of the simpler specular reflection used in the earlier version of RTTOV. The specular model is still used for water and ice covered surfaces (as this is considered more realistic).

² Cloud and aerosol scattering is modelled using the RTTOV 12 cloud and aerosol scattering coefficient files (see RD-29, RD-30). These contain spectral optical properties describing the optical depth, single scattering albedo and phase function of specific particulates (aerosol components such as dust, and sulfate; ice and liquid cloud as a function of effective diameter). For aerosol IMS fits the optical depth and layer height of coarse-mode dust aerosol and sulfate aerosol optical depth (assuming this to be in a layer around the tropopause, at zero relative humidity). In short-wave IASI channels, the radiative transfer uses the discrete ordinate solver (2 streams + single-scatter correction); in other channels (with negligible solar contribution the Chiu-scaling approximation is used, as described in the RTTOV user guide (RD-30).

 UKRI Science and Technology Facilities Council RAL Space	RAL IASI Methane Retrieval ATBD Version 2.1	2022-07-21
		Page 32 of 42

When using IMS-extended data the methane scheme also uses the IMS retrieved dust and sulfuric acid aerosol representation. This is expected to mitigate the impact of strong volcanic plumes on the methane retrieval (which has been noted for very large eruptions in the past such as Kasatochi in 2008 and Calbuco in 2015).

During the Methane+ project, a methane artefact over Venezuela was identified. The cause was traced to errors in the surface elevation data used by both IMS and the methane scheme (GTOPO30). The IMS and methane schemes were both updated to use GMTED2010 elevation data which corrected this feature (and some smaller artifacts in other locations).

 UKRI Science and Technology Facilities Council RAL Space	RAL IASI Methane Retrieval ATBD Version 2.1	2022-07-21
		Page 33 of 42

5.3 MEASUREMENTS

Following improvements to the forward model (see below), the full spectral range from 1232.25 to 1290 cm⁻¹ is now fitted (without any spectral gaps excluded).

Options to extend the spectral range towards 1330cm⁻¹ were also considered (see Figure 15). This would include stronger methane lines and bring more information on methane, especially at higher altitude. However, it was not possible to fit the full range consistently, implying that there remain significant errors in the spectroscopic data (or the line by line modelling). This conclusion is largely consistent with findings by a parallel ESA study on infra-red methane spectroscopy (RD-31). It is a clear priority for future work to evaluate the improved spectroscopic data which that study is expected to produce.

5.4 FORWARD MODEL

The version of RTTOV was upgraded to version 12, consistent with that used by IMS-extended. This enables cloud and aerosol to be represented in the methane scheme in a manner consistent with IMS-extended. Surface BRDF is also modelled as Lambertian over ice-free land as in IMS-extended.

The RTTOV coefficients were updated using RAL code to define the regression coefficients, based on new line-by-line transmittance calculations. Note (i) the predictors and training set of profiles are the same as those used by NWP-SAF to calculate the IASI coefficients supplied with RTTOV; (ii) Coefficients have to be re-computed by RAL to enable methane and water vapour isotopes to be modelled as variable gases. The new coefficients are improved as follows:


- Hitran 2018 data (downloaded from Hitran online in September 2020) [RD-25] is used. Previous coefficients were based on Hitran 2008.
- The line-by-line model LBLRTM [RD-24] is used (instead of the RFM). LBLRTM is able to model line mixing of methane in the band used here.
- 10 additional training profiles are added typical of scenes over desert (which are otherwise under-represented in the standard set of 83 profiles)
- An additional set of 83 profiles is added with methane profiles modified by quasi-random strongly vertically structured perturbation profiles. These introduce strong vertical structure into the methane profile variations, which helps to better constrain the regression and reduce spurious oscillations in RTTOV weighting functions. This leads to fewer artefacts in the averaging kernels produced by the retrieval (while not significantly changing the retrieved methane values themselves)

5.5 STATE VECTOR

5.5.1 SURFACE EMISSIVITY

A linear modification to the spectral surface emissivity from IMS is introduced into the methane fit. I.e. emissivity is modelled as:

$$\epsilon_i = \epsilon_i^{IMS} + f_0 + f_1(v_i - \bar{v})$$

 UKRI Science and Technology Facilities Council	RAL IASI Methane Retrieval ATBD Version 2.1	2022-07-21
		Page 34 of 42

Equation 18

Where ϵ_i is the modified emissivity in channel i ; ϵ_i^{IMS} is the emissivity from IMS; ν_i is the wavenumber of channel i ; $\bar{\nu}$ is the mean wavenumber in the fit window and f_0, f_1 are new fit parameters included in the retrieval state vector. Both are assumed to have *a priori* value of zero and *a priori* error 0.1.

This change leads to more successful retrievals over desert. Little benefit was found from fitting higher order spectral emissivity modifications.

5.5.2 SURFACE TEMPERATURE

Surface temperature is now assumed to be that from IMS (it is no longer retrieved).

5.5.3 METHANE A PRIORI

The same methane *a priori* profiles are used, however an extra term is added to the *a priori* covariance matrix to allow the retrieval freedom to effectively scale the entire profile. This is accomplished as follows:

$$C_{i,j} = C_{i,j}^{v2} + a_i \cdot a_j$$

Equation 19

Where

- $C_{i,j}$ is the new priori covariance between methane state vector elements i,j , expressed in units of vmr squared;
- $C_{i,j}^{v2}$ is the version 2 prior covariance value.
- a_i is the *a priori* vmr value at level i .

I.e. a fully correlated covariance representing 100% relative uncertainty in the profile is added to the version 2 covariance matrix. This allows the retrieval freedom to scale the entire methane profile, while retaining the previous constraint on variations in profile *shape*.

This change was introduced after finding that version 2 data tended to somewhat underestimate the methane trend from 2007 to 2020: The *a priori* profiles are approximately correct in 2009 but become increasingly negatively biased of the truth in later years. The new prior constraint is effective in reducing the influence of this systematically biased priori profile, yielding more realistic trends, without the need to introduce an explicit trend in the assumed prior methane profiles themselves. It is noted that using the new prior constraint introduces somewhat more noise (random error) into retrievals (as a natural consequence of the reduced smoothing) and this is particularly evident in situations where the methane signal is relatively low (e.g. at high latitudes).

5.6 ADDITIONAL MINOR TRACE GASES

The joint fitting of total column amounts the following minor gases was introduced into the retrieval: F14 (CF₄, carbon tetrafluoride), F22 (CHClF₂, Chloro(difluoro)methane), SO₂ (sulfur dioxide) and HNO₃ (nitric acid). This was implemented mainly because of the need to model the more highly variable of these (SO₂ and HNO₃) in tests where the fit window is extended up to 1330cm⁻¹. The spectral features of these gases are shown in Figure

15. Note that each of these gases is included, with a fixed assumed profile, in the RTTOV coefficients. In the methane retrieval a perturbation to the RTTOV modelled absorption is retrieved assuming the profile shape of the perturbation in mixing ratio is independent of altitude, and assuming that the perturbation in optical depth is optically thin. This is implemented as a linear correction to the RTTOV simulated radiance, using the derivative of radiance with respect to absorption coefficient .

As described in section 5.3, the extended wavelength range is not adopted in the candidate V3 scheme (due to methane spectroscopic inconsistencies). Nevertheless, all four minor gases are still fit, despite the extremely limited signal in the fit range up to 1290cm^{-1} .

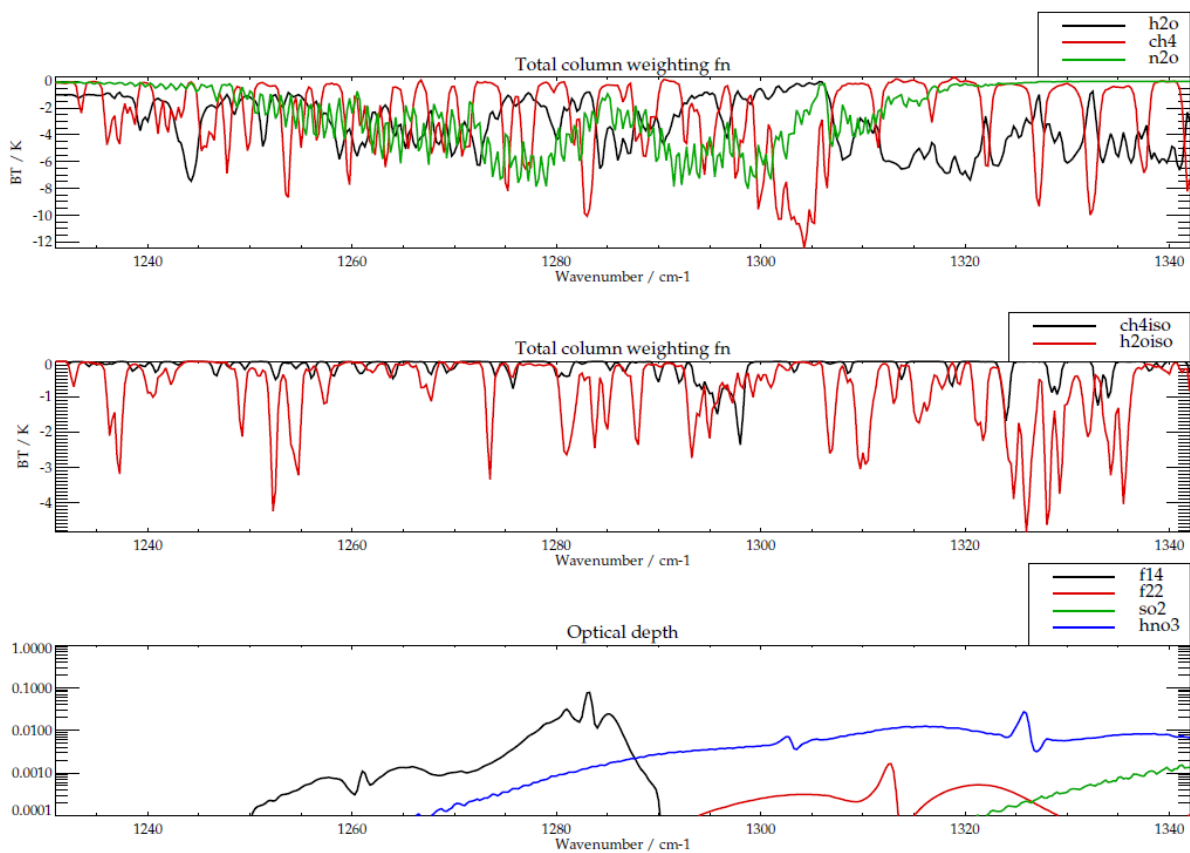



Figure 15: Illustration of trace gas spectral signatures in an extended fit window. The V2 retrieval uses the range $1232\text{-}1290\text{cm}^{-1}$. Tests were conducted to extend this range up to 1330cm^{-1} . Top panel shows brightness temperature (“BT” in Kelvin) weighting functions for total column perturbations of water vapour (“h2o”), methane (“ch4”) and nitrous oxide (“n2o”). Middle panel shows similar weighting functions for perturbations to all minor isotopes of methane (“ch4iso”) and water vapour (“h2oiso”). Bottom panel shows the total column (nadir) optical depths of F14, F22, sulfur dioxide (“so2”) and nitric acid (“hno3”). Profiles typical of mid-latitude observing conditions are assumed.

 UKRI Science and Technology Facilities Council	RAL IASI Methane Retrieval ATBD Version 2.1	2022-07-21
		Page 36 of 42

5.7 MODELLING N₂O

The N₂O profile is now defined using a combination of the new ACE-FTS version 4 climatology [RD-26], to define the stratosphere, and CAMS N₂O flux inversion data (Version 18r1) [RD-27] to define the profile in the troposphere. This version of CAMS data uses a 40 level hybrid sigma grid, with levels corresponding approximately to 0, 0.06, 0.13, 0.24, 0.39, 0.6, 0.88, 1.3, 1.7, 2.3, 3.1, 4, 5.1, 6.3, 7.7, 9, 10, 11, 12, 14, 15, 16, 17, 19, 20, 22, 24, 26, 28, 30, 33, 36, 38, 42, 45, 49, 53, 58, 65 km. The ACE data is defined on pressure levels corresponding approximately to 8.4, 9.6, 11, 12, 13, 14, 15, 16, 17, 18, 19, 21, 24, 27, 29, 32, 34, 37, 40, 43, 45, 48, 50, 53, 56, 59, 61, 64 (and further levels up to ~110km). The procedure below combines these profiles onto the more finely sampled RTTOV 101 level grid.

First the N₂O profile, $V_{ACE}(p)$, is defined using the updated ACE climatology, following the same approach as the V2 scheme, except that the N₂O trend is now assumed to be 0.296% year, updated based on NOAA GML data [ER-4] for the period 2007-end 2019.


Next, a profile, $V_{CAMS}(p)$, for the same time and location is constructed from the CAMS flux inversion data. In order to generally capture climatological spatial variations of N₂O, while also allowing the CAMS record to be simply extrapolated to IASI measurement times after the end of the available flux inversion data (end of 2018), the CAMS data is first processed to obtain mean profiles for each calendar month, considering all years from 2007-2018. These are averaged on the CAMS 1.875 x 3.75 degree latitude, longitude grid. To represent inter-annual variations (and trend), the global mean of each month in the same period is obtained. The monthly mean fields are normalised by the global mean value for the given month. This gives the mean relative spatial variation for a given calendar month, relative to the global mean for that month. To obtain the CAMS-derived N₂O profile for a given IASI observation we (i) interpolate the global mean time series to the time of the IASI observation (allowing linear extrapolation beyond the period covered by CAMS); (ii) interpolate the relative spatial variation field to the IASI location and multiply this by the global mean profile found for the time of the IASI measurement.

The combined CAMS and ACE N₂O profile $V_{CAMS+ACE}(p)$, is defined which uses CAMS in the troposphere and ACE in the stratosphere. The merging is carried out using the CAMS mixing ratio profile itself to determine the relative weight given to the two profiles (rather than explicitly identifying the tropopause). This exploits the fact that the N₂O mixing ratio profile is almost constant within the troposphere (and reduces, usually monotonically, in the stratosphere):

$$V_{CAMS+ACE}(p) = w(p)V_{CAMS}(p) + (1 - w(p))V_{ACE}(p)$$

Where

- $V_{CAMS}(p)$ is the CAMS mixing ratio profile (as function of pressure, p)
- $V_{ACE}(p)$ is the equivalent latitude / time interpolated ACE profile
- $w(p)$ is a weight from 0-1 which depends on the CAMS mixing ratio at the given level and the CAMS mixing ratio (in the same profile) at the surface, V_{TR} :
 - If $V_{CAMS}(p) \leq 0.9 * V_{TR}$, then $w(p)=0$
(i.e. the ACE profile is assumed at these levels)
 - If $V_{CAMS}(p) > 0.9 * V_{TR}$, then

 UKRI Science and Technology Facilities Council	RAL IASI Methane Retrieval ATBD Version 2.1	2022-07-21
		Page 37 of 42

$$w(p) = \frac{V_{CAM5}(p) - 0.9 * V_{TR}}{V_{TR} - 0.9 * V_{TR}}$$

I.e. at these levels, there is a linear interpolation (in CAMS vmr) between the two profiles.

The choice of the value 0.9 in the merging approach above is chosen somewhat empirically, noting that the N₂O variation from V_{TR} in the troposphere is reliable much smaller than 10%, so that, within the troposphere, the profile is dominated by CAMS and the merging mainly takes effect above the tropopause (where N₂O tends to monotonically decrease).

5.8 FITTING OF SYSTEMATIC RESIDUAL PATTERNS

Residual patterns are now derived as function of water vapour column as well as view geometry. In total four patterns are derived and the coefficient of each included in the retrieval state vector. The patterns are derived as follows:

- Modified retrievals are run for a reference day (15 July 2018) from Metop B measurements. The retrieval scheme used is the same as the version 3 scheme except as follows:
 - No residual patterns are modelled (and no coefficients are fit).
 - The methane profile shape is defined from a combination of ACE v4 data in the stratosphere and CAMS CH₄ flux inversion data in the troposphere (in a manner similar to that used to define the N₂O profile, described above). A scale factor for this methane profile shape is retrieved instead of the standard methane profile state vector.
- Considering only night-time retrievals, for scenes within a latitude range of 60S to 60N, fit residuals from this run are binned as a function of spectral channel, view zenith angle, θ , and total column water vapour, V_{H2O} (as retrieved in column average mixing ratio using).
- For each spectral channel (i), fit residuals patterns are determined via linear regression of the following function to the binned residual data:

$$\Delta y_i(\theta, V_{H2O}) = r_{0i} + \sec(\theta) (r_{1i} + r_{2i}V_{H2O} + r_{3i}V_{H2O}^2)$$

Equation 20

Where

- Δy_i is the mean residual for a given by of view zenith angle and total column water vapour.
- $r_{0i}, r_{1i}, r_{2i}, r_{3i}$ are the values of the residual patterns in channel i, found using linear regression to optimise the fit of the equation to the residuals in all view zenith and water vapour bins.

The resulting patterns are illustrated in Figure 16.

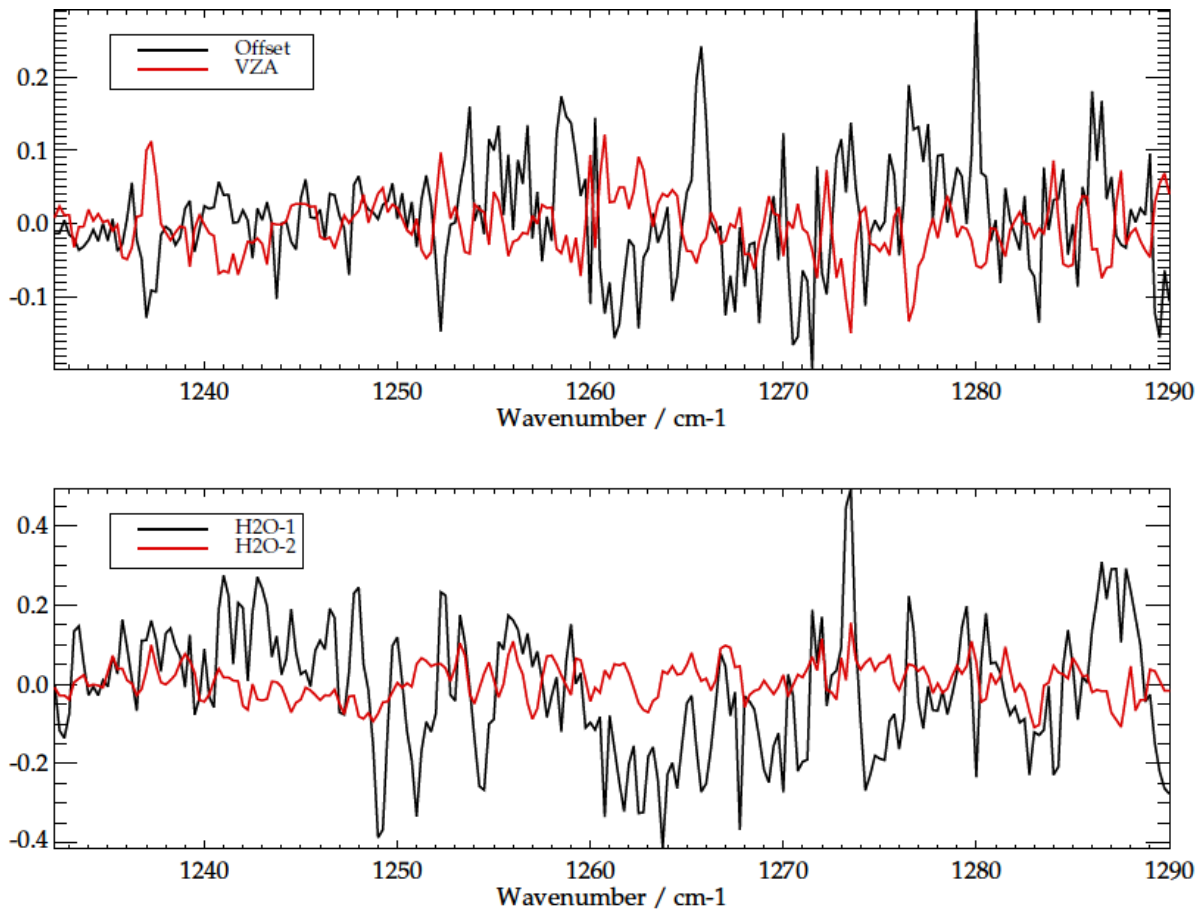



Figure 16: Systematic residual patterns used in the candidate v3 scheme (y axis units are Brightness temperature / K). These are derived from Metop B measurements on 15 July 2018. In the upper panel, the black line shows the fitted mean residual, while the red line shows the cross track dependent term. In the lower panel the lines show the first and second order water vapour patterns as described in the text.

 UKRI Science and Technology Facilities Council	RAL IASI Methane Retrieval ATBD Version 2.1	2022-07-21
		Page 39 of 42

6 L2 PRODUCT

6.1 OVERVIEW

Here we provide a brief description of the retrieval (L2) output files. More details on the practical use of the products is given in the product user guide (PUG) (RD-21). This includes important advice on quality control and on performing comparisons with independent data.

The format remains that of the previous version 1.0 product (to ensure compatibility with tools developed by previous users). Some additional variables are added to convey some potentially useful correlative information from the IMS retrieval (including a flag which indicates when the orbit is in ascending / descending node).

6.2 L2 FILE NAME

The filename format adheres to the following naming convention:

<institution>-<processing level>-<product>-<sensor>-<additional segregator>-<IASI orbit start time>Z_< IASI orbit end time >Z_<orbit section>-<version ID>.nc

E.g. ral-l2-ch4-iasi_metopa-tir_ims-20110629021455Z_20110629035654Z_000_049-v0200.nc

The segregators are defined as below:

- Institution: Indicator of where the data was processed, in this case “ral” for RAL.
- Processing level: e.g. L1, L2, L3, in this case “l2”.
- Product: The retrieved species, in this case “ch4”.
- Sensor: Instrument and platform, in this case “iasi_metopa”.
- Additional Segregator: To identify the algorithm, in this case “tir_ims”.
- IASI orbit start time: In the format YYYYMMDDhhmmss (UT). This is identical to date/time used in the original L1 file (for a full orbit).
- IASI orbit end time: as above.
- Orbit section: This contains the start and end scanline index within the L1 orbit. E.g. 000_049, 050_099, 100_149, 150_199, ...750_799. In this case “000_049”.
- Version ID: Version ID for the product, in this case “v0200”.

6.3 FORMAT AND CONTENT

6.3.1 DATA DIMENSIONS

The dataset dimensions are as described in Table 1, below.

Table 1: Dataset dimensions.

Dimension	Description	Value
pdim	Number of retrievals	Up to 1500
nmlev	Number of model levels	50
nrlev	Number of retrieval levels	12
adim	Number of methane retrieval levels for which averaging kernels are reported (only a subset to reduce the output file size)	5
rsfdim	Number of residual scale factors	2
edim	Number of emissivity values	3
apsfdim	Number of a priori scale factor values	1
al1dim	Number of AVHRR radiances	3
vdim	Number of off-diagonals (one half only) of the solution correlation matrix	66

6.3.2 GLOBAL ATTRIBUTES

Global attributes of the dataset are set as described in Table 2, below.

Table 2: Description of the output NetCDF global attributes.

Global Attribute	Description
creator_email	RAL RSG contact email address
project	Project name (NCEO)
licence	Details of data licence
platform	Satellite platform (MetOp-A)
sensor	Instrument on-board the satellite platform (IASI)
title	Dataset description (IASI offline thermal-IR methane retrievals)
product_version	Product release version (X.XX)
processor_version	Methane processor version (X.XX)
repository_version	Subversion repository number for methane processor IDL code
build_date	Date/time of code build used for processing (YYYY-MM-DDTHH:MM:SSZ)
processing_date	Date/time processing was performed (YYYY-MM-DDTHH:MM:SSZ)
date_created	Date/time NetCDF file was created (YYYY-MM-DDTHH:MM:SSZ)
institution	Creator institute (STFC Rutherford Appleton Laboratory)
input_file	Input IASI L1b file on the CEDA archive
history	Auxiliary retrieval setup information
input_ims_id	IMS pre-retrieval ID
input_ims_file	Input pre-processed IMS L2 file
time_coverage_start	Start date/time of IASI orbit file processed (YYYY-MM-DDTHH:MM:SSZ)
time_coverage_end	End date/time of IASI orbit file processed (YYYY-MM-DDTHH:MM:SSZ)
references	RAL RSG website reference (http://www.ralspace.stfc.ac.uk/remotesensing)
creator_name	RAL IASI products are developed with funding from the UK National Centre for Earth Observation
geospatial_lat_max	Maximum geospatial latitude within file

geospatial_lat_min	Minimum geospatial latitude within file
geospatial_lon_max	Maximum geospatial longitude within file
geospatial_lon_min	Minimum geospatial longitude within file
processing_status	Processing status (nominal)
conventions	CF compliance version (CF-1.6)

6.3.3 VARIABLES

Variable attributes of the dataset are described in Table 3, below.

Table 3: Description of the output NetCDF variable attributes. The retrieved methane profile and column, and their associated errors, are highlighted in light blue.

Variable	Units	Description	Dimensions
ak_vmr	1e-6	Averaging kernel for profile mixing ratios.	pdim, nmlev, adim
ak_xvmr	1e-6	Averaging kernel for column-averaged mixing ratio.	pdim, nmlev
ap_ch4iso_sf	-	Apriori 13CH4 scaling factor.	apsfdim
ap_ch4iso_sf_err	-	Apriori error on 13CH4 scaling factor.	apsfdim
ap_ch4_vmr	1e-6	A priori dry-air mole fraction of atmospheric methane (ppmv).	pdim, nrlev
ap_ch4_vmr_err	1e-6	A priori error on retrieved dry-air mole fraction of atmospheric methane (ppmv).	pdim, nrlev
ap_ch4_xvmr	1e-6	A priori column-averaged dry-air mole fraction of atmospheric methane (ppmv).	pdim
ap_ch4_xvmr_err	1e-6	A priori error on retrieved column-averaged dry-air mole fraction of atmospheric methane (ppmv).	pdim
ap_cloud_fraction	-	A priori effective cloud fraction.	pdim
ap_cloud_pressure	hPa	A priori effective cloud-top pressure (hPa).	pdim
ap_hdo_sf	-	Apriori HDO scaling factor.	apsfdim
ap_hdo_sf_err	-	Apriori error on HDO scaling factor.	apsfdim
ap_surface_temperature	K	A priori surface temperature (K).	pdim
bt_diff	K	The brightness temperature difference (K) at 12 microns between observations and simulations (based on ECMWF data). Used to initially screen observations for cloud.	pdim
ch4iso_sf	-	Retrieved 13CH4 scaling factor.	pdim
ch4iso_sf_err	-	Estimated error on retrieved 13CH4 scaling factor.	pdim
ch4_vmr	1e-6	Retrieved dry-air mole fraction of atmospheric methane (ppmv).	pdim, nrlev
ch4_vmr_err	1e-6	Estimated error on retrieved methane profile (ppmv).	pdim, nrlev
ch4_vsx		Off-diagonals of the solution correlation matrix for a subset of retrieval levels (as used for averaging kernels).	pdim, vdim
ch4_xvmr	1e-6	Retrieved column-averaged dry-air mole fraction of atmospheric methane (ppmv).	pdim
ch4_xvmr_eql	1e-6	Column-averaged equivalent CH4 (modelled).	pdim
ch4_xvmr_err	1e-6	Estimated error on the retrieved column-averaged mixing ratio (ppmv).	pdim
chim	-	Retrieval cost function value.	pdim
cloud_fraction	1	Retrieved effective cloud fraction.	pdim
cloud_pressure	hPa	Retrieved effective cloud-top pressure (hPa).	pdim
conv	-	Flag indicating retrieval convergence (1=fully converged). Results with other values should be used with more caution.	pdim
day	-	Day of the month (1-31).	pdim



ecmwf_alt	km	Spatially interpolated ECMWF surface altitude (km).	pdim
emis	1	Modelled surface spectral emissivity at selected wavenumbers.	pdim, edim
emis_wn	cm-1	Wavenumbers for which modelled surface spectral emissivity is provided.	edim
h2o_xvmr	1e-6	Retrieved column-averaged mole fraction of atmospheric water vapour in air (ppmv).	pdim
hdo_sf	-	Retrieved HDO scaling factor (effective HDO amount compared to HITRAN assumed ratio of HDO to main water vapour isotope).	pdim
hdo_sf_err	-	Estimated error on the retrieved HDO scaling factor.	pdim
iasi_alt	km	Surface altitude (km) corresponding to IASI measurement, based on averaging GTOPO30 to 12km resolution and sampling every 0.05 degrees.	pdim
ims_cloud_fraction	hPa	IMS (pre-retrieval) cloud fraction.	pdim
ims_cloud_pressure	hPa	IMS (pre-retrieval) cloud-top pressure.	pdim
ims_conv	-	IMS (pre-retrieval) retrieval convergence.	pdim
ims_dt1000	K	IMS (pre-retrieval) surface - 1000m air temperature difference.	pdim
ims_dt2	K	IMS (pre-retrieval) surface - 2m air temperature difference.	pdim
ims_iasc	-	IMS (pre-retrieval) flag indicating IASI ascending (1) or descending (0) node.	
ims_jx	-	IMS (pre-retrieval) retrieval cost function value (state vector component).	pdim
ims_jy	-	IMS (pre-retrieval) retrieval cost function value (measurement vector component).	pdim
ims_surface_temperature	K	IMS (pre-retrieval) surface temperature (K).	pdim
lat	degree_north	Latitude (degrees_north).	pdim
lon	degree_east	Longitude (degrees east).	pdim
mod_plev	hPa	Pressure levels of "true" state in provided averaging kernels.	nmlev
month	-	Month of the year (1-12).	pdim
n2o_xvmr_eql	1e-6	Column-averaged equivalent N2O (modelled)	pdim
nstep	-	The average number of retrieval steps (number of calls to the forward model).	pdim
pixel_number	-	IASI detector pixel (0-3).	pdim
rad_avhrr_tir	W/(m ² sr m ⁻¹)	AVHRR L1 (tir) radiances in channels 3b, 4 and 5.	pdim, al1dim
rad_avhrr_vis	W/(m ² sr)	AVHRR L1 (vis/nir/swir) radiances in channels 1, 2 and 3a.	pdim, al1dim
ret_plev	hPa	Retrieval pressure levels (hPa).	nrlev
ret_plev_ak	hPa	Pressures of retrieval levels (hPa) for which averaging kernels are provided.	adim
rsf	-	Scale factors for the mean fit and across-track residual patterns.	pdim, rsfdim
rsf_err	-	Errors on residual scale factors.	pdim, rsfdim
scan_line	-	Number of scan line (0=start of orbit).	pdim
scan_position	-	Position within scan line (0-29).	pdim
surface_pressure	hPa	Surface pressure (hPa) used in the retrieval.	pdim
surface_temperature	K	Retrieved surface temperature (K).	pdim
sza	degree	Solar zenith angle (degrees).	pdim
time_in_msec	msec	Time of day in msec since midnight (UTC).	pdim
vza	degree	Sensor zenith angle (degrees).	pdim
year	-	Year.	pdim